

neurons also responded to Oxt. In NG neurons isolated from *db/db* mice, by contrast, leptin failed to increase  $[Ca^{2+}]_i$  (Fig. 5B). Notably, Oxt evoked  $[Ca^{2+}]_i$  increases in these NG neurons of *db/db* mice (Fig. 5B), and the incidence and amplitude of  $[Ca^{2+}]_i$  responses to Oxt were indistinguishable between *db/db* and wild-type mice (Fig. 5, C and D). Thus Oxt activated leptin-resistant vagal afferent neurons of *db/db* mice.

Single ip injection of 200  $\mu\text{g}/\text{kg}$  Oxt into *db/db* mice significantly suppressed food intake for 0.5–3 h after injection to an extent similar to that in normal mice (Fig. 6A vs. Fig. 1A). We examined whether subchronic administration of Oxt for 2 wk using osmotic minipumps ameliorates hyperphagia in *db/db* mice. The surgery and implantation of osmotic minipumps markedly and transiently decreased daily food intake to a level around 2 g/day in saline and Oxt injection groups (Fig. 6B). The daily food intake largely recovered at day 2 after the surgery/implant and thereafter became stable through day 12 at the level around 6–8 g/day for saline and 4–6 g/day for Oxt (Fig. 6B). Thus subchronic Oxt treatment, compared with saline treatment, significantly reduced daily food intake for the period of day 2–12 and cumulative food intake for 12 days (Fig. 6C). Body weight gain at day 12 was  $-1.8 \pm 0.48$  g in saline-treated group and  $-3.2 \pm 0.29$  g in Oxt-treated group, showing a significant reduction of body weight by Oxt (Fig. 6D). The minus value of body weight gain at day 12 is suggested to be due to the transient decrease of daily food intake after surgery/implant. Thus peripheral Oxt injection activated vagal afferents, decreased food intake, and ameliorated obesity in obese *db/db* mice with leptin resistance.

## DISCUSSION

In the present study, ip administration of Oxt (200  $\mu\text{g}/\text{kg}$ ) suppressed food intake without evoking aversive behavior and induced c-Fos expression in NTS, and these effects were blunted in the mice treated with CAP or that received vagotomy. Oxt evoked membrane depolarization, action potential firings, and  $[Ca^{2+}]_i$  increases in the single NG neurons isolated from vagal afferents. The majority of the Oxt-responsive NG neurons also responded to CCK-8 and contained CART, both of which are known to inhibit feeding through vagal afferents. In Type 2 diabetic *db/db* mice, a model of leptin-resistant obesity, Oxt activated NG neurons, while leptin failed to do so. The results indicate that Oxt is able to activate NG neurons under leptin resistance, a condition characteristically associated with obesity. Moreover, peripheral subchronic Oxt infusion ameliorated hyperphagia and obesity in *db/db* mice. These results demonstrate that peripheral administration of Oxt, at least in pharmacological doses, suppresses food intake by activating vagal afferent NG neurons and subsequent signaling to the brain, and suggest that this peripheral Oxt-regulated vagal afferent route provides a novel tool to treat hyperphagia and obesity.

It has previously been shown that a fraction of NG neurons express the Oxt receptor mRNA and protein (52). In the present study, Oxt increased  $[Ca^{2+}]_i$  in isolated NG neurons, and this response was inhibited by Oxt receptor antagonist, indicating that Oxt activates vagal afferents via Oxt receptor. Approximately 15% of NG neurons responded to Oxt. This value (15%) of the incidence of Oxt-responsive vagal afferent neurons may be reasonable, due to the following consider-

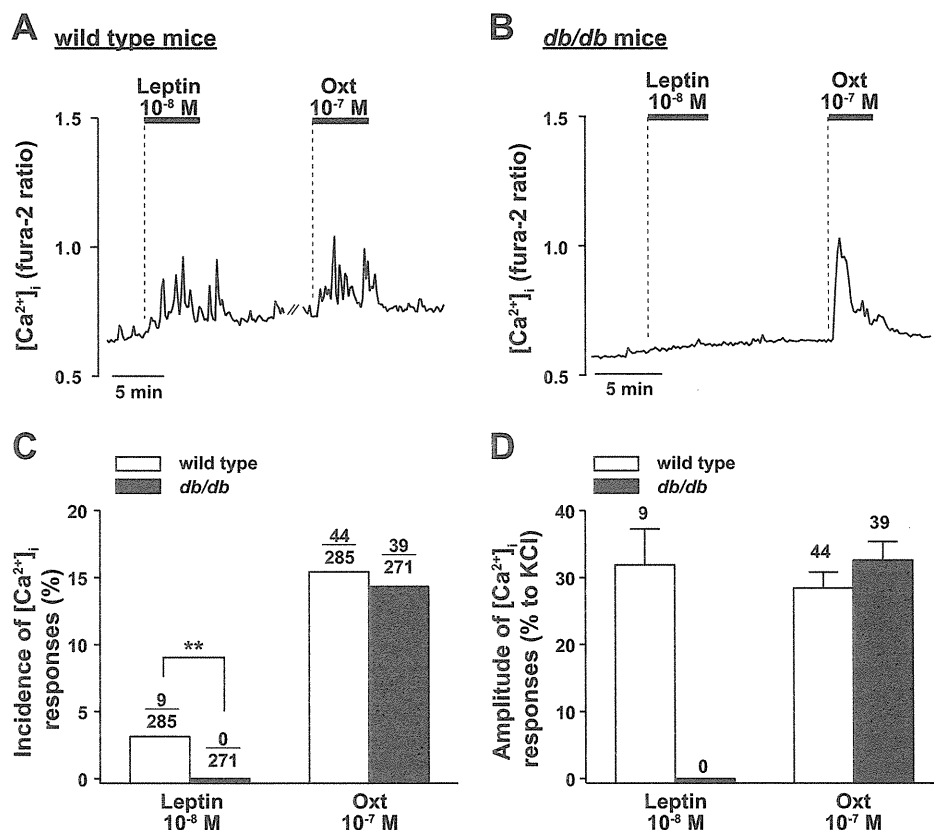


Fig. 5. Blunted leptin action but intact Oxt action to increase  $[Ca^{2+}]_i$  in NG neurons of obese diabetic *db/db* mice. **A:** leptin at  $10^{-8}$  M and Oxt at  $10^{-7}$  M increased  $[Ca^{2+}]_i$  in an isolated NG neuron of wild-type BKS mice ( $n = 9$ ). **B:** leptin failed to induce, but Oxt induced, an increase in  $[Ca^{2+}]_i$  in an NG neuron of *db/db* mice ( $n = 39$ ). **C and D:** incidence (**C**) and amplitude (**D**) of  $[Ca^{2+}]_i$  responses to leptin and Oxt in NG neurons of wild-type and *db/db* mice. **C:** numbers above each bar indicate the number of neurons that responded to each peptide over that responding to 55 mM KCl. **D:** numbers on each bar indicate number of neurons that responded to leptin or Oxt. Values are means  $\pm$  SE.  $**P < 0.01$  by  $\chi^2$  test.

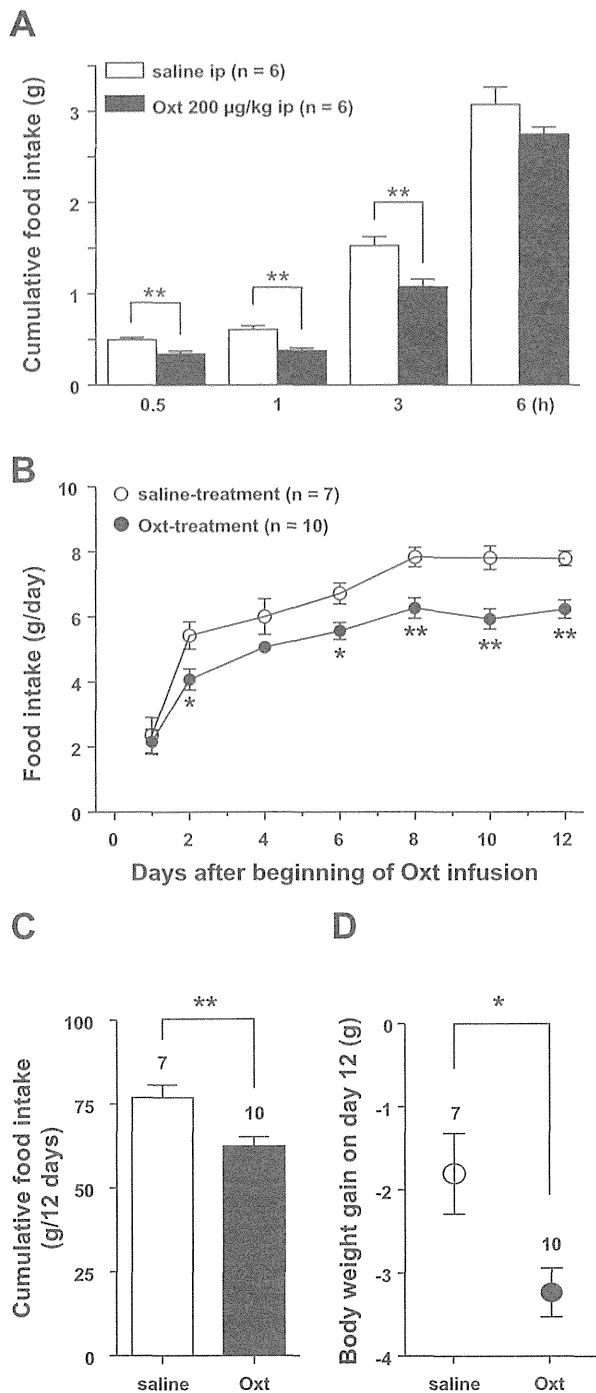


Fig. 6. Single and subchronic Oxt administrations decrease food intake and body weight in obese diabetic *db/db* mice. *A*: cumulative food intake after ip injection of saline (open bar) or Oxt (200 µg/kg, solid bar) in *db/db* mice. *B*: daily food intake during infusion of saline (open circle) or Oxt (1,600 µg·kg<sup>-1</sup>·day<sup>-1</sup>; solid circle) using osmotic minipump. Daily food intake markedly and transiently decreased possibly due to surgery and implant, followed by its substantial recovery on *day 2* and thereafter stable period. *C* and *D*: cumulative food intake for 12 days (*C*) and body weight gain on *day 12* of Oxt infusion (*D*). Values are means ± SE. \**P* < 0.05, \*\**P* < 0.01 vs. saline-group by unpaired *t*-test.

ations. First, vagal afferents innervate diverse tissues, forming many distinct subpopulations. A particular subpopulation that innervates a particular tissue could have a distinct ability of sensing specific factors. Second, peptide YY<sub>3-36</sub>, pancreatic polypeptide, and nesfatin-1, the hormones known to decrease food intake via interacting with vagal afferents, increase [Ca<sup>2+</sup>]<sub>i</sub> in ~10% of NG neurons (18, 19). Taken together, it is suggested that, among the highly heterogeneous NG neurons innervating diverse tissues and controlling a variety of functions, its particular subpopulation comprising 10~15% of total NG neurons has the ability to respond to a particular hormone.

The present study showed that Oxt induces action potential firings and increases [Ca<sup>2+</sup>]<sub>i</sub> in a subfraction of NG neurons that respond to CCK-8 and leptin. Previous studies showed that the NG neuron responses to CCK-8 and leptin are implicated in inhibition of feeding. CCK, released from enteroendocrine I cells in response to dietary nutrients (11), directly activates vagal afferent neurons via CCK-1 receptor (28, 45) and thereby rapidly decreases food intake (46). Leptin is produced by the stomach epithelial cells in addition to adipocytes (4). Leptin, released from the stomach in response to food and CCK (4), activates NG neurons of vagal afferents (40) and thereby inhibits food intake for a short time (41). Moreover, leptin receptor is co-expressed with CCK-1 receptor in NG neurons (29), and CCK and leptin synergistically activate NG neurons (40) and decrease food intake (5). These findings by us and others, taken together, suggest that the Oxt activation of CCK- and leptin-responsive NG neurons is linked to inhibition of food intake. Whether Oxt and leptin also cooperatively activate NG neurons and inhibit feeding remains to be studied.

We also found that Oxt activates NG neurons containing CART, a well-known neurotransmitter of vagal afferents (7). CART is co-expressed with CCK-1 and leptin receptors in NG neurons (7, 17), and CCK-8 and leptin stimulate expression and secretion of CART in NG neurons (9, 17). The anorexigenic effect of coadministration of CCK and leptin is blunted in the rats treated with CART small interfering RNA (17), suggesting that CART serves as a neurotransmitter in the NG neurons that respond to CCK and leptin. Accordingly, the Oxt-targeted, CCK- and leptin-responsive CART neurons in vagal afferents may play a role in regulation of feeding.

The anorexigenic effect of ip Oxt at 400 µg/kg in the early phase (0.5~1 h) was blunted by CAP treatment, whereas that in the later phase (3~6 h) significantly remained, indicative of vagal afferent-independent route. It has recently been reported that ip injection of Oxt (450~600 µg/kg) results in increased Oxt levels in the brain, including the hippocampus and amygdala (35), suggesting the transport of Oxt through BBB. Furthermore, the NTS, AP, and hypothalamic arcuate nucleus, the feeding-related areas, are considered to have leaky BBB and express Oxt receptors (54). Therefore, Oxt administered at a high dose (400 µg/kg) might significantly pass through BBB and act on the brain and thereby reduce feeding in the later period. However, further study is definitely needed to verify this possibility.

It remains unclear whether the anorexigenic effect of Oxt via vagal afferent pathway is pharmacological and/or plays a role in the normal regulation of daily food intake. Oxt is synthesized in the neurons in the hypothalamic PVN and SON, and released from the posterior pituitary to circulation. Plasma Oxt concentration is around 0.01~0.1 nM in rodents and humans (23, 38, 56) and is elevated by several times during delivery and lactation (24)

and postprandial periods (51). In the present study using single NG neurons, the effective concentration of Oxt to activate vagal afferents was around 0.1~100 nM (Fig. 1, A–D), ranging from the plasma Oxt level to its 1,000-fold higher level. Hence, the plasma Oxt, when elevated during lactation and postprandial periods, may act on a portion of vagal afferent neurons. It has been reported that ip administration of Oxt in a pharmacological dose (12 µg/mouse, around 450~600 µg/kg) results in plasma Oxt concentration around 1.5 nM (35), a dose capable of activating vagal afferent neurons in our study. Therefore, in our study, Oxt ip injection in pharmacological doses (200 and 400 µg/kg) may have reduced food intake, at least in part, via interacting with vagal afferents. More importantly, vagal afferents often terminate at the vicinity of hormone-secreting cells and sense higher concentrations of hormones in a paracrine fashion, as was previously proposed for CCK and insulin (20, 21, 42). This could also be the case for Oxt, in light of previous reports that Oxt is present in the uterus, testis, heart, pancreas, intestinal epithelium, and enteric nervous system (1, 24, 52). Moreover, ip injection of Oxt receptor antagonist was shown to induce hyperphagia during daytime in mice, suggesting that Oxt could regulate diurnal meal patterns (56). These findings by us and others suggest that endogenous Oxt in the periphery possibly interacts with the vagal afferents and regulate feeding. However, further studies are definitely required to verify the potential physiological role of the afferent vagal nerve in sensing Oxt in the circulation and/or peripheral tissues and in regulating feeding.

Obesity induces leptin resistance, a key factor that worsens obesity and leads to metabolic syndrome. Under leptin-resistant conditions, not only leptin itself, but also leptin-dependent agents, lose their ability to induce anorexigenic effect. Recent reports show that diet-induced obesity leads to leptin resistance in vagal afferents (8). Importantly, peripheral Oxt was shown to reduce food intake and body weight in DIO rats and mice (30, 33). The present study used the leptin-resistant obese *db/db* mice and examined the subchronic effect of Oxt released from implanted osmotic minipumps. The surgery and implantation of osmotic minipumps markedly and transiently decreased daily food intake. Daily food intake largely recovered at *day 2* and thereafter became stable. Oxt infusion resulted in significant reductions in the daily food intake during the stable phase and in body weight gain at *day 12*. The present study shows that peripheral subchronic infusion of Oxt decreases food intake and body weight, without aversive behavior. Previous reports show that peripheral Oxt induces no adverse effects on the locomotor activity (30) and blood pressure (30). Our present and previous results indicate that the activation of vagal afferents by peripheral Oxt injection provides a promising tool to treat hyperphagia and obesity. In addition, the vagal afferent-mediated pathway could possibly serve as a signaling route of Oxt for treatment of autism (53), although further study is required to address this issue.

#### ACKNOWLEDGMENTS

The authors thank Dr. Yukari Date at University of Miyazaki and Dr. Shuichi Koda at Asubio Pharma for advice on vogotomy. We thank Kaori Tsubonoya, Chizu Sakamoto, Minako Warashina, Seiko Ookuma, Miyuki Kondo, Megumi Motoshima, Atsumi Shinozaki, and Yuka Hobo at Jichi Medical University for technical assistance.

#### GRANTS

This work was supported by Grant-in-Aid for Young Scientist (B) (22790218, 24790221) from Japan Society for the Promotion of Science (JSPS), Jichi Medical University Young Investigator Award, and The Naito Foundation to Y. Iwasaki. A part of this study was supported by Grant-in-Aid for Scientific Research (C) (24591341) and Scientific Research on Innovative Areas (23126523) from JSPS, Memorial Foundation for Female Natural Scientists, and Kowa Life Science Foundation to Y. Maejima. This work was supported by Grant-in-Aid for Scientific Research (B) (23390044) and for Challenging Exploratory Research (26670453) from JSPS, Strategic Research Program for Brain Sciences (10036069) by the Ministry of Education, Culture, Sports, Science and Technology of Japan (MEXT), MEXT-Supported Programs for Strategic Research Foundation at Private Universities 2011–2015 (Cooperative Basic and Clinical Research on Circadian Medicine) and 2013–2017, Health Labor Sciences Research Grants from the Ministry of Health, Labor, and Welfare, Japan, a grant from Japan Diabetes Foundation, and a grant from Salt Science Research Foundation (no. 1434) to T. Yada. This study was subsidized by JKA through its promotion funds from KEIRIN RACE to T. Yada.

#### DISCLOSURES

No conflicts of interest, financial or otherwise, are declared by the author(s).

#### AUTHOR CONTRIBUTIONS

Author contributions: T.Y., Y.I., and Y.M. conception and design of research; Y.I., Y.M., S.S., M.Y., T.A., K.K., P.K., and M.K. performed experiments; T.Y., Y.I., Y.M., S.S., and M.K. analyzed data; T.Y., Y.I., Y.M., H.N., and M.K. interpreted results of experiments; T.Y., Y.I., Y.M., and M.K. prepared figures; T.Y., Y.I., and S.S. drafted manuscript; T.Y., Y.I., S.S., and M.K. edited and revised manuscript; T.Y. and Y.I. approved final version of manuscript.

#### REFERENCES

- Amico JA, Finn FM, Haldar J. Oxytocin and vasopressin are present in human and rat pancreas. *Am J Med Sci* 296: 303–307, 1988.
- Arletti R, Benelli A, Bertolini A. Influence of oxytocin on feeding behavior in the rat. *Peptides* 10: 89–93, 1989.
- Arletti R, Benelli A, Bertolini A. Oxytocin inhibits food and fluid intake in rats. *Physiol Behav* 48: 825–830, 1990.
- Bado A, Levasseur S, Attoub S, Kermorgant S, Laigneau JP, Bortoluzzi MN, Moizo L, Lehy T, Guerre-Millo M, Le Marchand-Brustel Y, Lewin MJ. The stomach is a source of leptin. *Nature* 394: 790–793, 1998.
- Barrachina MD, Martinez V, Wang L, Wei JY, Tache Y. Synergistic interaction between leptin and cholecystokinin to reduce short-term food intake in lean mice. *Proc Natl Acad Sci USA* 94: 10455–10460, 1997.
- Bergquist F, Ludwig M. Dendritic transmitter release: a comparison of two model systems. *J Neuroendocrinol* 20: 677–686, 2008.
- Broberger C, Holmberg K, Kuhar MJ, Hokfelt T. Cocaine- and amphetamine-regulated transcript in the rat vagus nerve: a putative mediator of cholecystokinin-induced satiety. *Proc Natl Acad Sci USA* 96: 13506–13511, 1999.
- de Lartigue G, Barbier de la Serre C, Espero E, Lee J, Raybould HE. Diet-induced obesity leads to the development of leptin resistance in vagal afferent neurons. *Am J Physiol Endocrinol Metab* 301: E187–E195, 2011.
- De Lartigue G, Dimaline R, Varro A, Raybould H, De la Serre CB, Dockray GJ. Cocaine- and amphetamine-regulated transcript mediates the actions of cholecystokinin on rat vagal afferent neurons. *Gastroenterology* 138: 1479–1490, 2010.
- Deblon N, Veyrat-Durebex C, Bourgoin L, Caillon A, Bussier AL, Petrosino S, Piscitelli F, Legros JJ, Geenen V, Foti M, Wahli W, Di Marzo V, Rohner-Jeanrenaud F. Mechanisms of the anti-obesity effects of oxytocin in diet-induced obese rats. *PLoS One* 6: e25565, 2011.
- Dockray GJ. Cholecystokinin and gut-brain signalling. *Regul Pept* 155: 6–10, 2009.
- Donaldson ZR, Young LJ. Oxytocin, vasopressin, and the neurogenetics of sociality. *Science* 322: 900–904, 2008.
- Gallego R, Eyzaguirre C. Membrane and action potential characteristics of A and C nodose ganglion cells studied in whole ganglia and in tissue slices. *J Neurophysiol* 41: 1217–1232, 1978.
- Garami A, Balasko M, Szekeley M, Solymar M, Petervari E. Fasting hypometabolism and refeeding hyperphagia in rats: effects of capsaicin desensitization of the abdominal vagus. *Eur J Pharmacol* 644: 61–66, 2010.

15. Gimpl G, Fahrenholz F. The oxytocin receptor system: structure, function, and regulation. *Physiol Rev* 81: 629–683, 2001.
16. Hamilton RB, Norgren R. Central projections of gustatory nerves in the rat. *J Comp Neurol* 222: 560–577, 1984.
17. Heldsinger A, Lu Y, Zhou SY, Wu X, Grabauskas G, Song I, Owyang C. Cocaine- and amphetamine-regulated transcript is the neurotransmitter regulating the action of cholecystokinin and leptin on short-term satiety in rats. *Am J Physiol Gastrointest Liver Physiol* 303: G1042–G1051, 2012.
18. Iwasaki Y, Kakei M, Nakabayashi H, Ayush EA, Hirano-Kodaira M, Maejima Y, Yada T. Pancreatic polypeptide and peptide YY<sub>3–36</sub> induce Ca<sup>2+</sup> signaling in nodose ganglion neurons. *Neuropeptides* 47: 19–23, 2013.
19. Iwasaki Y, Nakabayashi H, Kakei M, Shimizu H, Mori M, Yada T. Nesfatin-1 evokes Ca<sup>2+</sup> signaling in isolated vagal afferent neurons via Ca<sup>2+</sup> influx through N-type channels. *Biochem Biophys Res Commun* 390: 958–962, 2009.
20. Iwasaki Y, Shimomura K, Kohno D, Dezaki K, Ayush EA, Nakabayashi H, Kubota N, Kadowaki T, Kakei M, Nakata M, Yada T. Insulin activates vagal afferent neurons including those innervating pancreas via insulin cascade and ca influx: its dysfunction in IRS2-KO mice with hyperphagic obesity. *PLoS One* 8: e67198, 2013.
21. Iwasaki Y, Yada T. Vagal afferents sense meal-associated gastrointestinal and pancreatic hormones: mechanism and physiological role. *Neuropeptides* 46: 291–297, 2012.
22. Johnstone LE, Fong TM, Leng G. Neuronal activation in the hypothalamus and brainstem during feeding in rats. *Cell Metab* 4: 313–321, 2006.
23. Kagerbauer SM, Martin J, Schuster T, Blobner M, Kochs EF, Landgraf R. Plasma oxytocin and vasopressin do not predict neuropeptide concentrations in human cerebrospinal fluid. *J Neuroendocrinol* 25: 668–673, 2013.
24. Kiss A, Mikkelsen JD. Oxytocin-anatomy and functional assignments: a minireview. *Endocr Regul* 39: 97–105, 2005.
25. Koda S, Date Y, Murakami N, Shimbara T, Hanada T, Toshinai K, Nijima A, Furuya M, Inomata N, Osuye K, Nakazato M. The role of the vagal nerve in peripheral PYY<sub>3–36</sub>-induced feeding reduction in rats. *Endocrinology* 146: 2369–2375, 2005.
26. Kohno D, Nakata M, Maejima Y, Shimizu H, Sedbazar U, Yoshida N, Dezaki K, Onaka T, Mori M, Yada T. Nesfatin-1 neurons in paraventricular and supraoptic nuclei of the rat hypothalamus coexpress oxytocin and vasopressin and are activated by refeeding. *Endocrinology* 149: 1295–1301, 2008.
27. Kublaoui BM, Gemelli T, Tolson KP, Wang Y, Zinn AR. Oxytocin deficiency mediates hyperphagic obesity of Sim1 haploinsufficient mice. *Mol Endocrinol* 22: 1723–1734, 2008.
28. Lankisch TO, Tsunoda Y, Lu Y, Owyang C. Characterization of CCK<sub>A</sub> receptor affinity states and Ca<sup>2+</sup> signal transduction in vagal nodose ganglia. *Am J Physiol Gastrointest Liver Physiol* 282: G1002–G1008, 2002.
29. Li Y, Wu X, Zhou S, Owyang C. Low-affinity CCK-A receptors are coexpressed with leptin receptors in rat nodose ganglia: implications for leptin as a regulator of short-term satiety. *Am J Physiol Gastrointest Liver Physiol* 300: G217–G227, 2011.
30. Maejima Y, Iwasaki Y, Yamahara Y, Kodaira M, Sedbazar U, Yada T. Peripheral oxytocin treatment ameliorates obesity by reducing food intake and visceral fat mass. *Aging (Albany NY)* 3: 1169–1177, 2011.
31. Maejima Y, Sedbazar U, Suyama S, Kohno D, Onaka T, Takano E, Yoshida N, Koike M, Uchiyama Y, Fujiwara K, Yashiro T, Horvath TL, Dietrich MO, Tanaka S, Dezaki K, Oh IS, Hashimoto K, Shimizu H, Nakata M, Mori M, Yada T. Nesfatin-1-regulated oxytocinergic signaling in the paraventricular nucleus causes anorexia through a leptin-independent melanocortin pathway. *Cell Metab* 10: 355–365, 2009.
32. Mens WB, Witter A, van Wimersma Greidanus TB. Penetration of neurohypophyseal hormones from plasma into cerebrospinal fluid (CSF): half-times of disappearance of these neuropeptides from CSF. *Brain Res* 262: 143–149, 1983.
33. Morton GJ, Thatcher BS, Reidberger RD, Ogimoto K, Wolden-Hanson T, Baskin DG, Schwartz MW, Blevins JE. Peripheral oxytocin suppresses food intake and causes weight loss in diet-induced obese rats. *Am J Physiol Endocrinol Metab* 302: E134–E144, 2012.
34. Nelson EE, Alberts JR, Tian Y, Verbalis JG. Oxytocin is elevated in plasma of 10-day-old rats following gastric distension. *Brain Res Dev Brain Res* 111: 301–303, 1998.
35. Neumann JD, Maloumy R, Beiderbeck DI, Lukas M, Landgraf R. Increased brain and plasma oxytocin after nasal and peripheral administration in rats and mice. *Psychoneuroendocrinology* 38: 1985–1993, 2013.
36. Olson BR, Hoffman GE, Sved AF, Stricker EM, Verbalis JG. Cholecystokinin induces c-fos expression in hypothalamic oxytocinergic neurons projecting to the dorsal vagal complex. *Brain Res* 569: 238–248, 1992.
37. Onaka T, Takayanagi Y, Yoshida M. Roles of oxytocin neurones in the control of stress, energy metabolism, and social behaviour. *J Neuroendocrinol* 24: 587–598, 2012.
38. Onaka T, Yagi K. Oxytocin release from the neurohypophysis after the taste stimuli previously paired with intravenous cholecystokinin in anaesthetized rats. *J Neuroendocrinol* 10: 309–316, 1998.
39. Patel JD, Ebenezer IS. The effect of intraperitoneal administration of leptin on short-term food intake in rats. *Eur J Pharmacol* 580: 143–152, 2008.
40. Peters JH, Karpel AB, Ritter RC, Simasko SM. Cooperative activation of cultured vagal afferent neurons by leptin and cholecystokinin. *Endocrinology* 145: 3652–3657, 2004.
41. Peters JH, McKay BM, Simasko SM, Ritter RC. Leptin-induced satiation mediated by abdominal vagal afferents. *Am J Physiol Regul Integr Comp Physiol* 288: R879–R884, 2005.
42. Peters JH, Ritter RC, Simasko SM. Leptin and CCK selectively activate vagal afferent neurons innervating the stomach and duodenum. *Am J Physiol Regul Integr Comp Physiol* 290: R1544–R1549, 2006.
43. Renaud LP, Tang M, McCann MJ, Stricker EM, Verbalis JG. Cholecystokinin and gastric distension activate oxytocinergic cells in rat hypothalamus. *Am J Physiol Regul Integr Comp Physiol* 253: R661–R665, 1987.
44. Rinaman L, Rothe EE. GLP-1 receptor signaling contributes to anorexigenic effect of centrally administered oxytocin in rats. *Am J Physiol Regul Integr Comp Physiol* 283: R99–R106, 2002.
45. Simasko SM, Wiens J, Karpel A, Covasa M, Ritter RC. Cholecystokinin increases cytosolic calcium in a subpopulation of cultured vagal afferent neurons. *Am J Physiol Regul Integr Comp Physiol* 283: R1303–R1313, 2002.
46. Smith GP, Jerome C, Cushin BJ, Eterno R, Simansky KJ. Abdominal vagotomy blocks the satiety effect of cholecystokinin in the rat. *Science* 213: 1036–1037, 1981.
47. Talsania T, Anini Y, Siu S, Drucker DJ, Brubaker PL. Peripheral exendin-4 and peptide YY<sub>3–36</sub> synergistically reduce food intake through different mechanisms in mice. *Endocrinology* 146: 3748–3756, 2005.
48. Tomizawa K, Iga N, Lu YF, Moriwaki A, Matsushita M, Li ST, Miyamoto O, Itano T, Matsui H. Oxytocin improves long-lasting spatial memory during motherhood through MAP kinase cascade. *Nat Neurosci* 6: 384–390, 2003.
49. Tung YC, Ma M, Piper S, Coll A, O’Rahilly S, Yeo GS. Novel leptin-regulated genes revealed by transcriptional profiling of the hypothalamic paraventricular nucleus. *J Neurosci* 28: 12419–12426, 2008.
50. Ueta Y, Kannan H, Higuchi T, Negoro H, Yamaguchi K, Yamashita H. Activation of gastric afferents increases noradrenaline release in the paraventricular nucleus and plasma oxytocin level. *J Auton Nerv Syst* 78: 69–76, 2000.
51. Verbalis JG, McCann MJ, McHale CM, Stricker EM. Oxytocin secretion in response to cholecystokinin and food: differentiation of nausea from satiety. *Science* 232: 1417–1419, 1986.
52. Welch MG, Tamir H, Gross KJ, Chen J, Anwar M, Gershon MD. Expression and developmental regulation of oxytocin (OT) and oxytocin receptors (OTR) in the enteric nervous system (ENS) and intestinal epithelium. *J Comp Neurol* 512: 256–270, 2009.
53. Yamasue H, Yee JR, Hurlmann R, Rilling JK, Chen FS, Meyer-Lindenberg A, Tost H. Integrative approaches utilizing oxytocin to enhance prosocial behavior: from animal and human social behavior to autistic social dysfunction. *J Neurosci* 32: 14109–14117, 2012.
54. Yoshida M, Takayanagi Y, Inoue K, Kimura T, Young LJ, Onaka T, Nishimori K. Evidence that oxytocin exerts anxiolytic effects via oxytocin receptor expressed in serotonergic neurons in mice. *J Neurosci* 29: 2259–2271, 2009.
55. Zhang G, Bai H, Zhang H, Dean C, Wu Q, Li J, Guariglia S, Meng Q, Cai D. Neuropeptide exocytosis involving synaptotagmin-4 and oxytocin in hypothalamic programming of body weight and energy balance. *Neuron* 69: 523–535, 2011.
56. Zhang G, Cai D. Circadian intervention of obesity development via reting-stage feeding manipulation or oxytocin treatment. *Am J Physiol Endocrinol Metab* 301: E1004–E1012, 2011.

# Nasal Oxytocin Administration Reduces Food Intake without Affecting Locomotor Activity and Glycemia with c-Fos Induction in Limited Brain Areas

Yuko Maejima<sup>a, b</sup> Rauza Sukma Rita<sup>a</sup> Putra Santoso<sup>a</sup> Masato Aoyama<sup>c</sup>  
Yuichi Hiraoka<sup>d</sup> Katsuhiko Nishimori<sup>d</sup> Darambazar Gantulga<sup>a</sup>  
Kenju Shimomura<sup>a, b</sup> Toshihiko Yada<sup>a, e</sup>

<sup>a</sup>Division of Integrative Physiology, Department of Physiology, Jichi Medical University School of Medicine, Shimotsuke, <sup>b</sup>Department of Electrophysiology and Oncology, Fukushima Medical University School of Medicine, Fukushima, <sup>c</sup>Department of Animal Science, Faculty of Agriculture, Utsunomiya University, Utsunomiya, <sup>d</sup>Department of Molecular and Cell Biology, Graduate School of Agricultural Science, Tohoku University, Miyagi, and <sup>e</sup>Division of Adaptation Development, Department of Developmental Physiology, National Institute for Physiological Sciences, Okazaki, Japan

## Key Words

Oxytocin · Nasal treatment · Paraventricular nucleus · Dorsal motor nucleus of vagus · Glucose tolerance · Obesity · Insulin release

## Abstract

Recent studies have considered oxytocin (Oxt) as a possible medicine to treat obesity and hyperphagia. To find the effective and safe route for Oxt treatment, we compared the effects of its nasal and intraperitoneal (IP) administration on food intake, locomotor activity, and glucose tolerance in mice. Nasal Oxt administration decreased food intake without altering locomotor activity and increased the number of c-Fos-immunoreactive (ir) neurons in the paraventricular nucleus (PVN) of the hypothalamus, the area postrema (AP), and the dorsal motor nucleus of vagus (DMNV) of the medulla. IP Oxt administration decreased food intake and locomotor activity and increased the number of c-Fos-ir neurons not only in the PVN, AP, and DMNV but also in the nucleus of

solitary tract of the medulla and in the arcuate nucleus of the hypothalamus. In IP glucose tolerance tests, IP Oxt injection attenuated the rise of blood glucose, whereas neither nasal nor intracerebroventricular Oxt affected blood glucose. In isolated islets, Oxt administration potentiated glucose-induced insulin secretion. These results indicate that both nasal and IP Oxt injections reduce food intake to a similar extent and increase the number of c-Fos-ir neurons in common brain regions. IP Oxt administration, in addition, activates broader brain regions, reduces locomotor activity, and affects glucose tolerance possibly by promoting insulin secretion from pancreatic islets. In comparison with IP administration, the nasal route of Oxt administration could exert a similar anorexigenic effect with a lesser effect on peripheral organs.

© 2015 S. Karger AG, Basel

Yuko Maejima and Rauza Sukma Rita contributed equally to this work.

## Introduction

Oxytocin (Oxt) is a neurohypophysial hormone that regulates uterine contraction during labor and milk ejection [1]. Oxt is synthesized in the paraventricular (PVN) and supraoptic nucleus of the hypothalamus. It is released peripherally after being shuttled to the pituitary [2], or centrally in the brain to regulate neuronal process [3]. Recent studies have clarified new functions of Oxt in the central nervous system, including increased trust [4], regulation of social recognition [5] and development of mother-infant bonding [6]. In addition, our previous study employed Oxt in the PVN-driven anorexigenic circuit in rats [7].

The anorexigenic effect of Oxt has been reported since the early 1990s. Olson et al. [8] showed that Oxt and its agonist decrease food intake when administered centrally in rats, and Arletti et al. [9] showed that intracerebroventricular (icv) injection of Oxt inhibits food intake together with water intake. More recent studies have shown that mice with deficient Oxt or Oxt receptor (Oxt-R) develop late-onset obesity [10, 11].

Obesity is linked to numerous diseases including type 2 diabetes, cardiovascular events, and certain forms of cancer [12, 13]. Several antiobesity drugs, including diethylpropion, fenproporex, mazindol, fluoxetine, and sibutramine, have been developed [14], but there is little evidence for effective and safe treatments.

We have previously shown that subchronic peripheral Oxt treatment through a subcutaneously implanted osmotic minipump reduces hyperphagia and obesity in high-fat diet-fed obese mice, and that intraperitoneal (IP) Oxt treatment similarly reduces hyperphagia [15]. Zhang et al. [16] have recently reported that the nasal administration of Oxt decreases body weight (BW) in obese subjects. Ott et al. [17] showed that nasal Oxt treatment reduces reward-driven food intake. These reports indicate that subcutaneous, IP, and nasal routes of Oxt treatment have common actions of reducing obesity and hyperphagia. However, a comparison of these actions and underlying mechanisms following different administration routes of Oxt has not been previously undertaken.

We performed a comparative study on the effects of nasal and IP administration of Oxt on feeding, locomotor activity, and glucose tolerance in mice, and found that both nasal and IP Oxt injections reduce food intake to a similar extent with increased c-Fos-immunoreactive (ir) neurons in common brain regions. IP Oxt administration also increased c-Fos-ir neurons in additional brain re-

gions, reduced locomotor activity, and affected glucose tolerance possibly by promoting insulin secretion from pancreatic islets.

## Materials and Methods

### Animals

Male C57BL/6J mice (aged 6 weeks) were obtained from Japan SLC (Hamamatsu, Japan). Animals were maintained on a 12-hour light/dark cycle. The dark and light phases started at 19:30 h and 7:30 h, respectively. Mice were allowed ad libitum access to water and a standard diet (CE-2; Clea, Osaka, Japan). Experimental procedures and care of animals were carried out according to the Jichi Medical University Institute of Animal Care and Use Committee. The mice used in the experiments were well habituated to minimize stress.

### Measurements of Food Intake and Locomotor Activity after Oxt Administration

Following deprivation of food for 2 h before the dark phase, the animals received 0.1–10  $\mu\text{g}/10 \mu\text{l}$  nasal Oxt or 40 and 400  $\mu\text{g}/\text{kg}$  IP Oxt (Peptide Institute, Osaka, Japan) 30 min before the dark phase. For the nasal administration, 10  $\mu\text{l}$  of Oxt or vehicle was dropped into the nasal cavity. Cumulative food intake was measured for the following 0.5, 1, 2, 6, and 24 h. For the measurements during the dark phase, red light with minimum intensity was used to prevent mice from being stimulated by bright light. Locomotor activity was measured by an activity monitoring system (ACTIMO-100; Shinfactory, Fukuoka, Japan). The doses of nasal Oxt were 0.1, 1 and 10  $\mu\text{g}$ , based on the minimum effective dose of Oxt (1  $\mu\text{g}$ ) on food intake determined by pilot experiments. The dose of IP Oxt was based on a previous report [15] showing that 400  $\mu\text{g}/\text{kg}$  Oxt markedly and long-lastingly suppressed food intake.

### Immunostaining of c-Fos after Oxt Administration

Food was deprived for 2 h before the dark phase until perfusion. The animals received nasal (1  $\mu\text{g}/10 \mu\text{l}$ ) or IP Oxt (400  $\mu\text{g}/\text{kg}$ ) administration 30 min before the dark phase. After 90 min, the mice were transcardially perfused as described previously [7]. Coronal sections of 40- $\mu\text{m}$  thickness were cut with a freezing microtome. Sections at 120- $\mu\text{m}$  intervals between -0.58 and -8.0 mm from the bregma were used for c-Fos immunohistochemistry. Sections were rinsed in phosphate-buffered saline (PBS; 0.01 M, pH 7.4), incubated in PBS containing 2% normal goat serum and 2% bovine serum albumin (BSA), then incubated with rabbit anti-c-Fos antiserum (sc-52, 1:5,000; Santa Cruz, Calif., USA). Subsequently, the sections were incubated with biotinylated goat anti-rabbit IgG (1:500; Vector Laboratories Inc., Calif., USA), and an avidin-biotin complex (ABC kit; Vector Laboratories Inc.). Immunoreactions were visualized by incubating in diaminobenzidine (DAB) solution containing nickel ammonium.

Bilateral sections of the hypothalamus and brainstem between -0.58 and -8.0 mm from the bregma were prepared, with c-Fos-ir cells per section counted manually under the microscope. The cell count per section was averaged for all sections in each investigated nucleus of each animal.

### Glucose Tolerance Test and Measurement of Plasma Insulin

Mice aged 10 weeks (or with a BW of 22–25 g) were cannulated in the lateral ventricle (0.5 mm caudal to bregma, 1.0 mm lateral from the midline, and 2.2 mm below the skull surface; ICM-23G09 Inter Medical, Osaka, Japan) and housed individually. BW and food intake were not significantly different before the operation and for 10 days thereafter. On the day of the experiment, food was deprived at 09:00 h and an IP glucose tolerance test (IPGTT; 2 g/kg) was started at 13:00 h. IPGTT was performed 20 min after nasal (0.1, 1, 10  $\mu\text{g}$ ), icv (0.4, 4  $\mu\text{g}$ ) or IP (40, 400  $\mu\text{g}/\text{kg}$ ) Oxt injection. Oxt doses for icv injection were determined based on our previous report [7]. Blood was sampled by cutting the surface of the tail skin under local anesthesia with EMLA cream (AstraZeneca K.K., London, UK) without restraint. Blood glucose levels were measured using Glucocard (Arkray, Kyoto, Japan).

For the measurement of plasma insulin, mice aged 10 weeks (22–26 g BW) were used. IP Oxt injection (400  $\mu\text{g}/\text{kg}$ ) and IPGTT procedures followed the same protocol and time course. The mice were decapitated, and their blood was collected 10 min after IPGTT. After centrifugation, plasma insulin concentration was measured by ultrasensitive mouse insulin ELISA kit (Morinaga Institute of Biological Science, Inc., Yokohama, Japan).

### Isolation of Islets and Measurement of Insulin Secretion

Mice with similar age and BW to those in the IPGTT were used. Islets were isolated as previously described [18] and cultured overnight in DMEM solution (Sigma, St. Louis, Mo., USA). After 30 min of preincubation in 2 mM glucose solution and 30 min under static incubation conditions in Krebs-Ringer Buffer (mM): 120 NaCl, 4.7 KCl, 2.5  $\text{CaCl}_2$ , 1  $\text{KH}_2\text{PO}_4$ , 1.2  $\text{MgSO}_4$ , 10 HEPES, 25  $\text{NaHCO}_3$ , pH 7.4 (with NaOH), plus 0.1% BSA, experimental glucose (2, 5, 20 mM) with or without Oxt (10 nM), insulin secretion was measured. Islets were then incubated overnight at  $-20^\circ\text{C}$  with acidified ethanol solution (95% ethanol, 5% acetic acid) to extract all insulin. Insulin was measured using a Morinaga mouse ELISA kit (Morinaga Institute of Biological Science, Inc.).

### Statistical Analysis

All data are presented as means  $\pm$  SEM. The statistical analysis of experimental data of c-Fos-ir neurons, insulin secretion, and plasma insulin were carried out using Student's *t* test. Data for food intake, locomotor activity, and glucose tolerance test were analyzed by repeated measures of two-way ANOVA with treatment (saline vs. Oxt including dose responses) and time as factors. Post hoc multiple comparisons were made using Tukey's test. Significance was set at  $p < 0.05$  for all analyses.

## Results

### Effect of Oxt Administration on Food Intake and Locomotor Activity

In order to compare the effects of nasal and IP Oxt administration, we administered an approximately equally effective amount of Oxt for nasal and IP administration (nasal: 0.1–10  $\mu\text{g}/25$  g BW, i.e. approx. 4–400  $\mu\text{g}/\text{kg}$ ; IP: 40–400  $\mu\text{g}/\text{kg}$ ). Nasal administration of Oxt at

doses of 0.1–10  $\mu\text{g}/10$   $\mu\text{l}$  was performed in mice weighing 20–25 g. These doses correspond to approximately 4–400  $\mu\text{g}/\text{kg}$ .

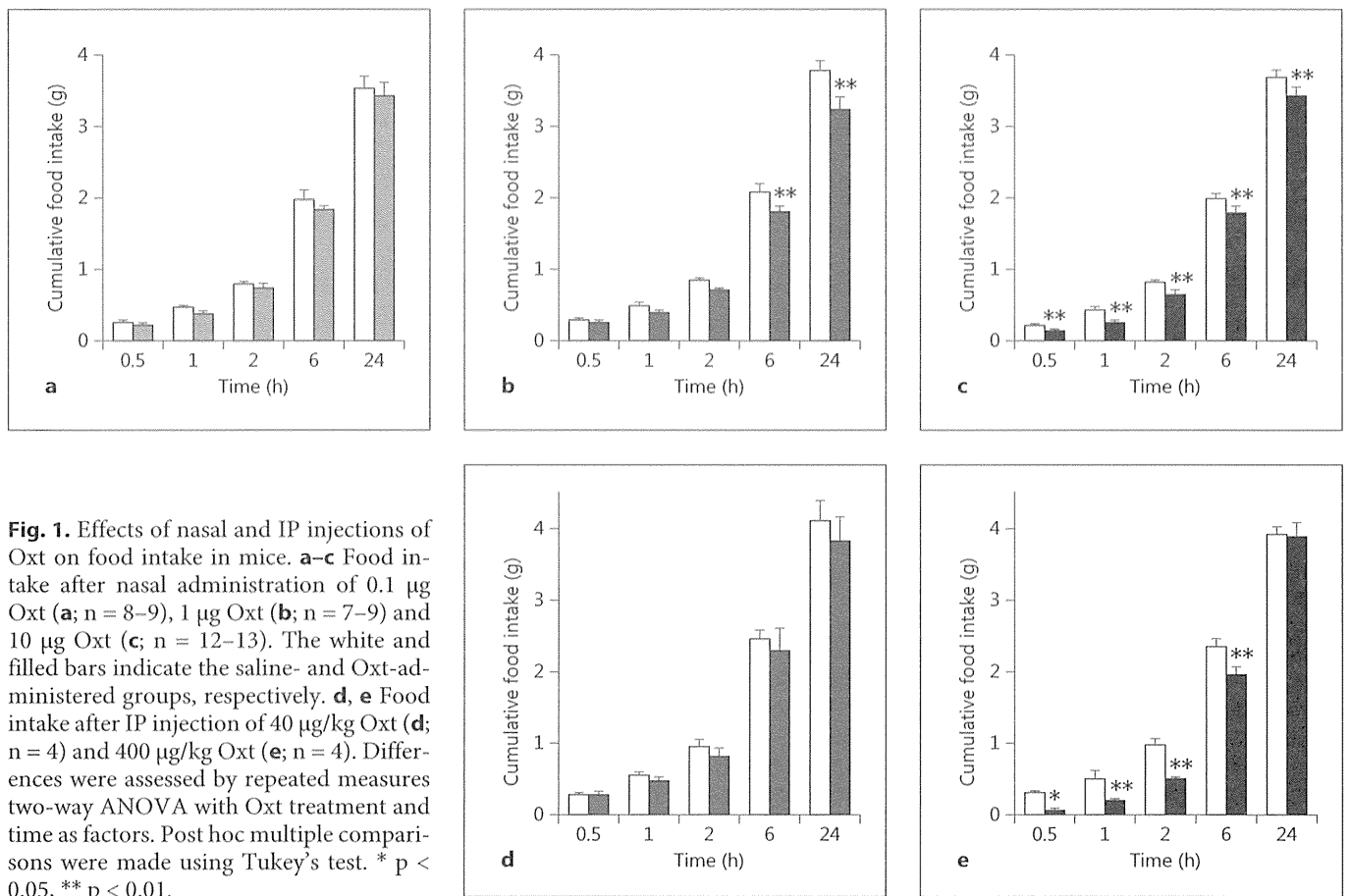
Nasal administration of 0.1  $\mu\text{g}$  Oxt did not affect the food intake significantly ( $F_{1,60} = 2.53$ ,  $p > 0.05$ ; fig. 1a). Administration of 1  $\mu\text{g}$  Oxt significantly decreased the food intake ( $F_{1,56} = 27.4$ ,  $p < 0.01$ ; fig. 1b), and 10  $\mu\text{g}$  Oxt ( $F_{1,92} = 27.16$ ,  $p < 0.01$ ; fig. 1c). Tukey's test indicated that nasal administration of 1  $\mu\text{g}$  Oxt reduced the cumulative food intake 6 and 24 h after administration (fig. 1b), and 10  $\mu\text{g}$  Oxt reduced the food intake 0.5, 1, 2, 6, and 24 h after administration (fig. 1c) without changing locomotor activity ( $F_{1,299} = 0.10$ ,  $p > 0.05$ ; fig. 2a, c).

IP administration of 40  $\mu\text{g}/\text{kg}$  Oxt failed to significantly affect the food intake ( $F_{1,24} = 2.27$ ,  $p > 0.05$ ; fig. 1d) and 400  $\mu\text{g}/\text{kg}$  Oxt markedly decreased the food intake at 0.5, 1, 2, and 6 h ( $F_{1,24} = 38.9$ ,  $p < 0.01$ ; fig. 1e) but not at 24 h. IP injection of 400  $\mu\text{g}/\text{kg}$  Oxt showed a tendency to decrease locomotor activity ( $F_{1,138} = 2.6$ ,  $p > 0.05$ ) for the first 7 h and significantly decreased cumulative locomotor activity during the dark phase (fig. 2b, d).

The tendency and time course of reduction in the food intake were similar between nasal and IP administration (fig. 1b, d). However, at a higher dose (approx. 400  $\mu\text{g}/\text{kg}$ ), nasal administration of Oxt (10  $\mu\text{g}/\mu\text{l}$ ; fig. 1c) reduced the cumulative food intake for up to 24 h, but the extent of food intake reduction during 0.5–6 h was smaller compared to IP administration (fig. 1e).

### Effect of Oxt Administration on the Number of c-Fos-ir Neurons

After nasal administration of 1  $\mu\text{g}$  Oxt, the number of c-Fos-ir neurons was significantly increased in the PVN of the hypothalamus. The number was  $137.1 \pm 25.6/\text{section}$  in controls versus  $284.6 \pm 37.4/\text{section}$  in Oxt-injected groups ( $p < 0.05$ ; fig. 3a, b, e). Nasal Oxt administration also increased the number of c-Fos-ir neurons in the medulla, the area postrema (AP;  $10.6 \pm 3.5/\text{section}$  in controls vs.  $27.3 \pm 4.7/\text{section}$  in Oxt-injected groups), and the dorsal motor nucleus of vagus (DMNV;  $32.3 \pm 6.9/\text{section}$  in controls vs.  $69.2 \pm 4.7/\text{section}$  in Oxt-injected groups; fig. 3c–e). IP administration of Oxt also increased the number of c-Fos-ir neurons in the PVN ( $71.7 \pm 18.1/\text{section}$  in controls vs.  $188.0 \pm 35.2/\text{section}$  in Oxt-injected groups), DMNV ( $14.7 \pm 3.7/\text{section}$  in controls vs.  $43.4 \pm 4.8/\text{section}$  in Oxt-injected groups; fig. 3f, g, j), nucleus of the solitary tract (NTS;  $39.5 \pm 9.8/\text{section}$  in controls vs.  $153.3 \pm 6.0/\text{section}$  in Oxt-injected groups), and the arcuate nucleus (ARC;  $68.9 \pm 12.2/\text{section}$  in control vs.  $128.6 \pm 7.0$  in Oxt groups), consistent with our previous



report [15]. Thus, IP but not nasal administration of Oxt increased c-Fos-ir neurons in the NTS and ARC.

#### Effect of Oxt Administration on Glucose Metabolism

The effect of Oxt on the elevated levels of blood glucose during IPGTT was examined. Nasal and icv Oxt administration had no effect on blood glucose levels in IPGTT ( $F_{3,84} = 0.28$ ,  $p > 0.05$ , and  $F_{2,54} = 1.02$ ,  $p > 0.05$ , respectively; fig. 4a, c). In contrast, IP administration of 40 and 400 µg/kg Oxt ( $F_{2,36} = 13.10$ ,  $p < 0.01$ ) dose-dependently attenuated the elevation of blood glucose at 30 and 60 min of IPGTT (fig. 4b). The alteration of glycemia prompted us to examine whether Oxt affects insulin release from pancreatic islets. Ten minutes after IPGTT, plasma insulin concentration was significantly increased ( $2.19 \pm 0.26$  ng/ml), compared with the saline-injected group ( $0.93 \pm 0.12$  ng/ml; fig. 4d). Incubation of isolated islets with 10 nM Oxt-enhanced insulin secretion in the stimulatory (20 mM), but not in the low (2 mM) and basal (5 mM) glucose conditions (fig. 4e).

#### Discussion

It has recently been reported that nasal administration of Oxt reduces BW in obese humans [17]. To the best of our knowledge, the present study is the first to show the effect of nasal Oxt in reducing food intake in rodents without affecting locomotor activity or blood glucose level. This may suggest a selective anorexigenic action of nasal treatment of Oxt.

Neumann et al. [19] reported the increase of brain and plasma Oxt concentrations after nasal administration in rats and mice. The dose (12 µg/10 µl) and application method used in their study are almost identical to those used here (10 µg/10 µl). Hence, we speculate that Oxt levels in the brain and plasma may have been increased after nasal administration of Oxt in the present study. Nasal administration of Oxt may lead to its inhalation into the lungs [20], thereby increasing the plasma Oxt level. If so, pharmacokinetics of Oxt may be similar between nasal and IP applications. Hence, the similar anorexigenic effects of



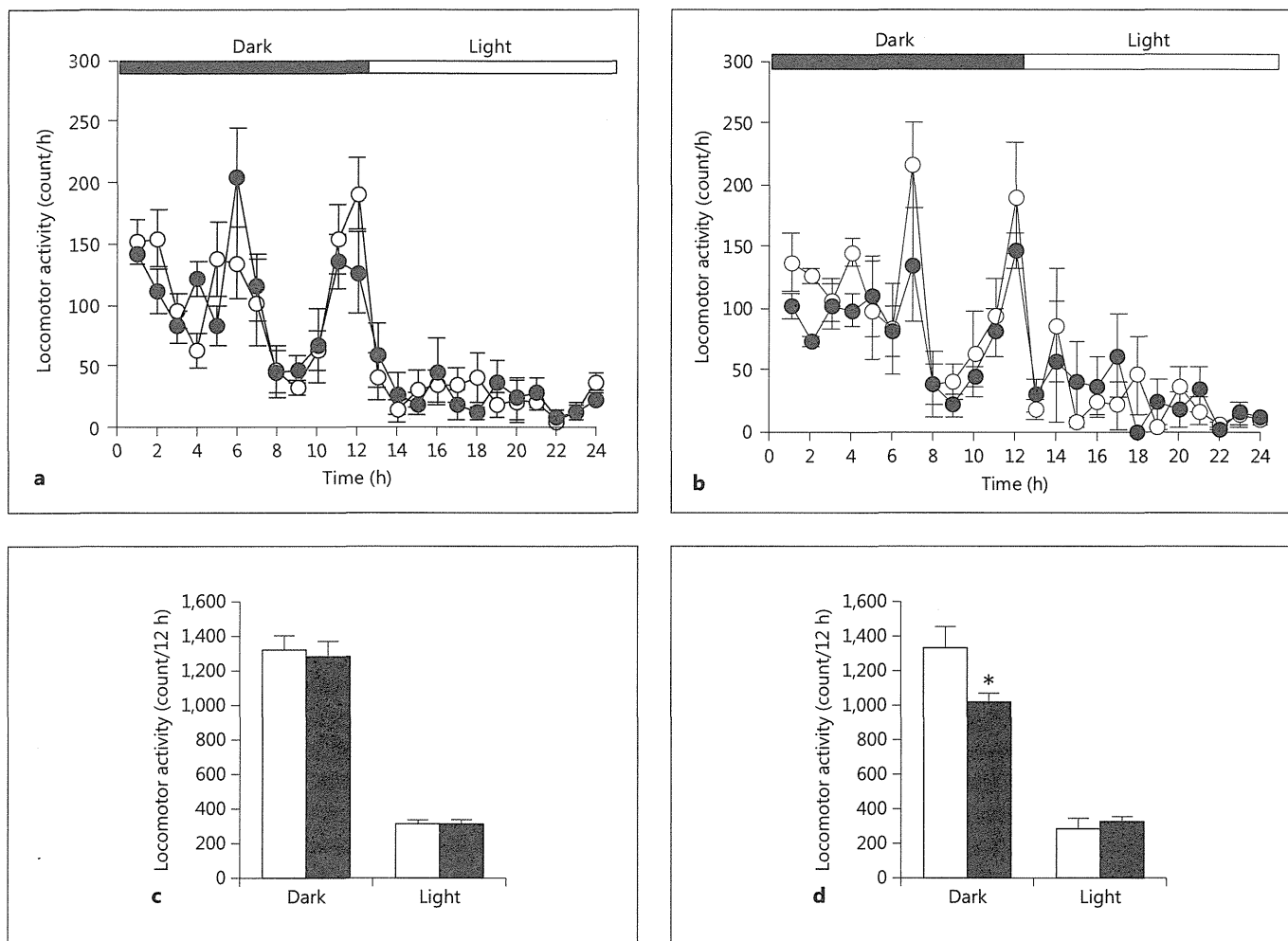


**Fig. 2.** Effects of nasal and IP injections of Oxt on locomotor activity in mice. **a, b** Locomotor activity for every 1 h during the 24-hour period after nasal administration of 10 µg Oxt ( $n = 7-8$ ; **a**) and IP administration of 400 µg/kg Oxt ( $n = 4$ ; **b**). Nasal and IP administration of Oxt was performed just before the dark phase. Empty and full circles indicate the control and Oxt-injected groups, respectively. Differences were assessed by repeated mea-

asures of two-way ANOVA with Oxt treatment and time as factors. Post hoc multiple comparisons were made using Tukey's test. \*  $p < 0.05$ . **c, d** Cumulative locomotor activity after nasal (**c**) and IP administration of Oxt (**d**). Open and solid bars indicate the control and Oxt-injected groups. Differences were assessed by Student's *t* test.

nasal and IP Oxt treatments shown in the present study may have been mediated largely by the increase of peripheral Oxt concentration. In addition, Oxt is reported to cross the blood-brain barrier (BBB) from the blood to the brain by 0.05% [21]. The permeation of Oxt through the BBB depends on the concentration of Oxt in vessels. Since our study used a high dose of Oxt via nasal and IP routes, a significant amount of the peptide may have reached the central nervous system by crossing the BBB [3, 22].

On the other hand, this study has shown that both nasal and IP administration of Oxt induces *c-Fos* in PVN,

AP, and DMNV. In addition, only IP administration of Oxt induces *c-Fos* in ARC and NTS.

In apparent discrepancy with our results, nasal administration of Oxt (1 µg) has been reported to have no effect on *c-Fos*-ir neurons in rats [23]. However, this discrepancy may be explained by the dose of Oxt. In the study by Ludwig et al. [23], the dose of Oxt used was 1 µg for rats (BW: 250–300 g). In the present study, it was 1 µg for mice (BW: 25–30 g), a factor 10 times higher when corrected for BW. Oxt doses that induced *c-Fos* in the present study correspond to 1–100 times of the total Oxt content of ap-

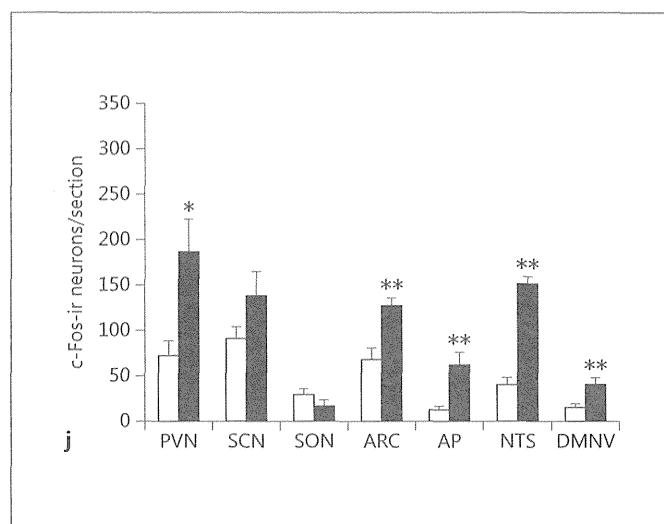
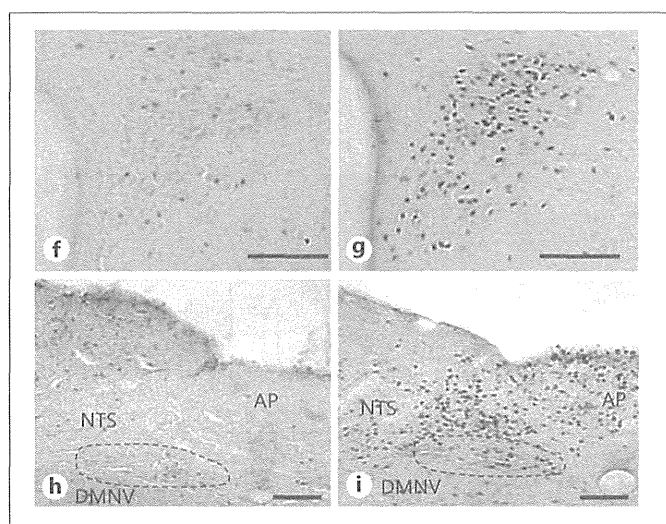
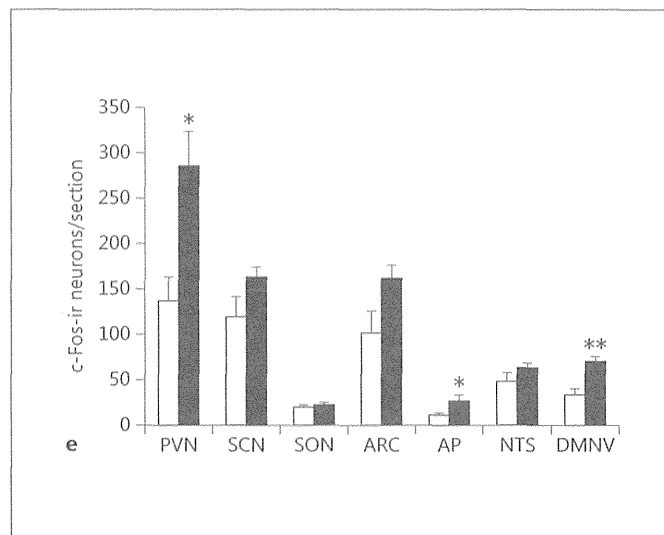
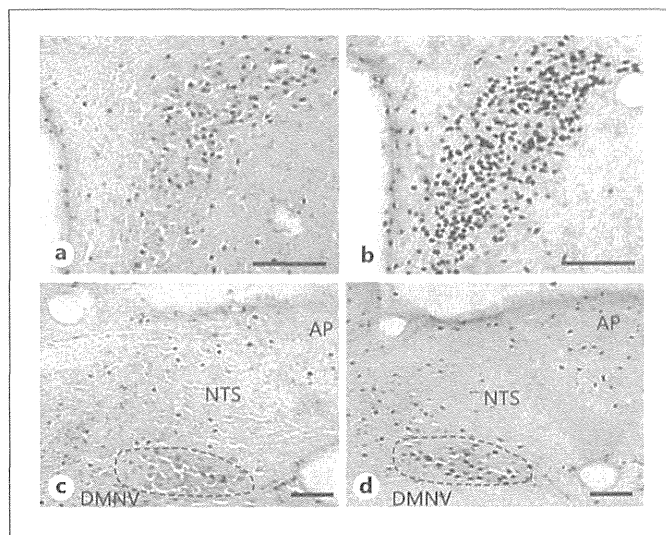


**Fig. 3.** c-Fos-ir neurons after nasal and IP Oxt injection. **a–d** Microphotographs of c-Fos-ir neurons in the PVN (**a, b**) and dorsal vagal complex (**c, d**) after nasal administration of saline (**a, c**) or 1 µg Oxt (**b, d**). **e** Number of c-Fos-ir neurons after nasal administration of Oxt in feeding-related areas in the hypothalamus and brain stem (n = 4). **f–i** Microphotographs of c-Fos-ir neurons in

PVN (**f, g**) and dorsal vagal complex (**h, i**) after IP injection of saline (**f, h**) or 400 µg/kg Oxt (**g, i**). **j** Number of c-Fos-ir neurons after IP injection of Oxt in feeding-related areas (n = 4). Scale bars = 100 µm. Differences were assessed for significance by Student's t test. \* p < 0.05, \*\* p < 0.01. SCN = Suprachiasmatic nucleus; SON = supraoptic nucleus.

proximately 150 ng in the mouse pituitary [24]. Hence, it is suggested that a relatively high dose of nasal Oxt is required to induce c-Fos expression. In addition, the present study used a higher dose of Oxt (approx. 10 µg nasal, approx. 400 µg/kg IP) than that used in a human study (approx. 48 µg nasal) [17]. The different dose requirement between humans and rodents is possibly due to different anatomical structures and/or to the different approach for nasal Oxt administration between humans

(vaporizer or nasal spray) and mice (dropping the Oxt-containing solution on the nose by a pipette).

In this study, Oxt administration via the nasal versus the IP route increased the number of c-Fos-ir neurons in both common and distinct brain areas. Both nasal and IP administration of Oxt increased c-Fos-ir neurons in the PVN, AP, and DMNV. The increase in the PVN may underlie the common action of nasal and IP Oxt administration to suppress food intake, since PVN is recognized as

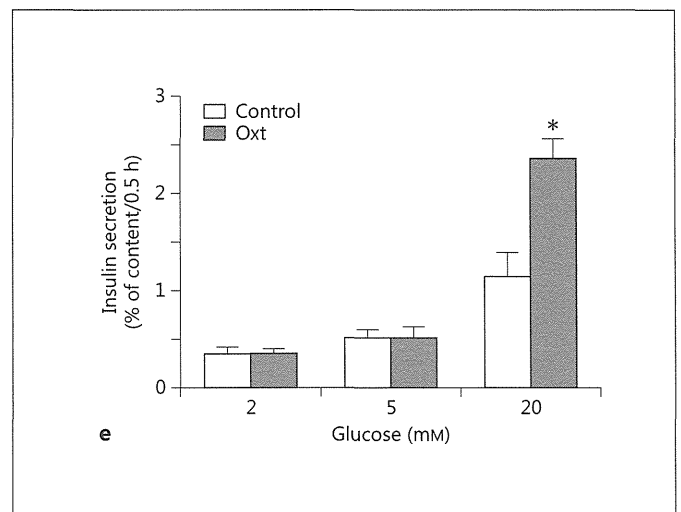
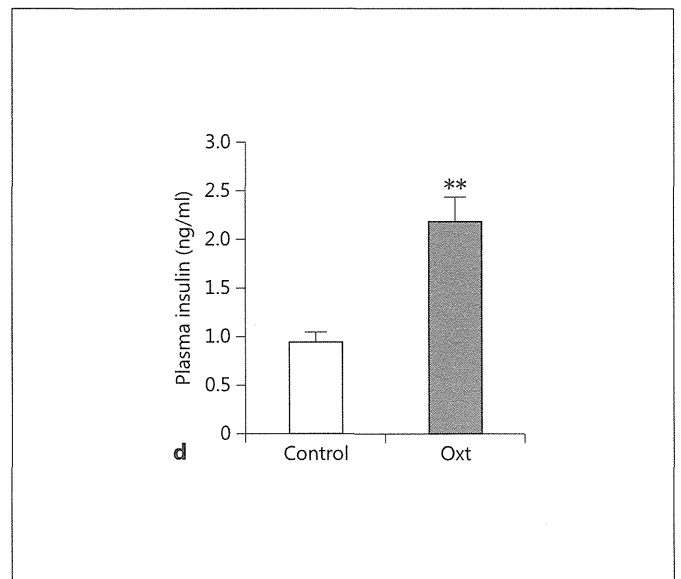
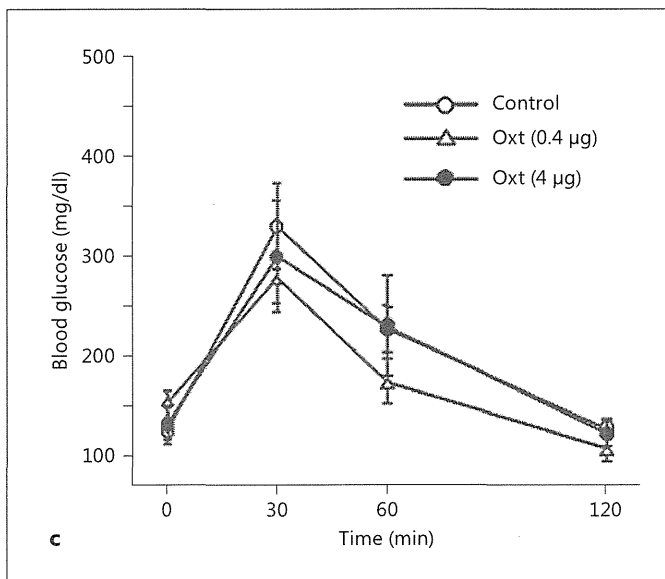
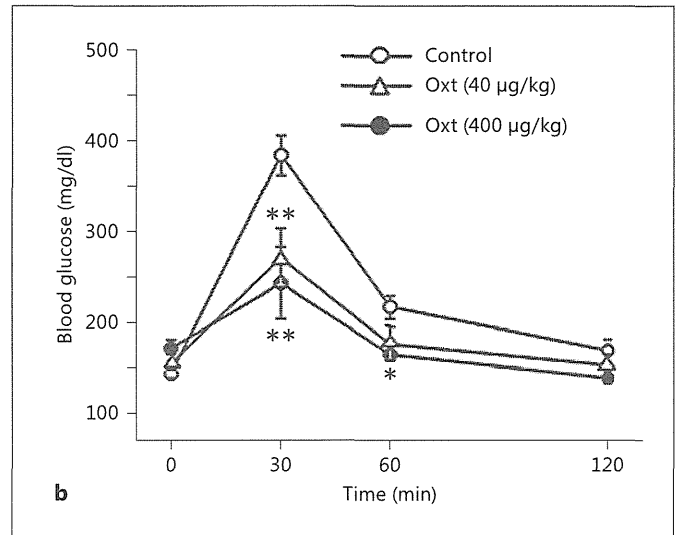
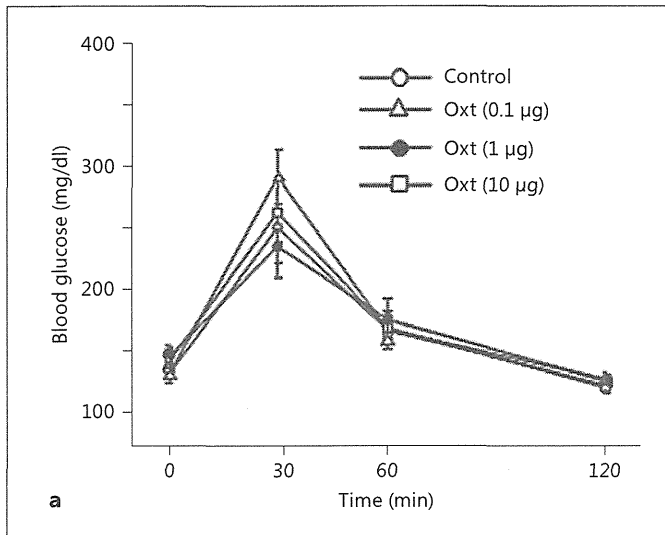


**Fig. 4.** Effect of Oxt on blood glucose levels in glucose tolerance test and insulin levels. **a–c** Blood glucose profiles in IPGTT after Oxt administration via nasal (0.1, 1, and 10 µg; n = 6–11; **a**), IP (40 and 400 µg/kg; n = 5; **b**) and icv administration (0.4 and 4 µg; n = 5–8; **c**). Differences were assessed by repeated measures two-way ANOVA with Oxt treatment and time as factors. For each time point, post hoc multiple comparisons were made using Tukey's test. \*  $p < 0.05$ , \*\*  $p < 0.01$  versus control. **d** Plasma insulin levels after IP administration of Oxt. \*\*  $p < 0.01$ . **e** Insulin secretion from isolated pancreatic islets under static incubation with low (2 mM), basal (5 mM), and stimulatory (20 mM) glucose concentrations. Open bars indicate the control group (n = 11) and solid bars indicate the Oxt-treated group (n = 11). Differences were assessed for significance by Student's t test. \*  $p < 0.05$ .

an integrative center for feeding and energy metabolism [25, 26]. The neurons in the ARC of the hypothalamus sense various nutrients and hormones and convey neural information to the neurons in PVN, where peripheral and central information is integrated [27]. In contrast, only IP Oxt increased c-Fos-ir neurons in the ARC and NTS. Several pathways may be considered for the common and distinct brain signalling by nasal and IP Oxt. First, given that the cribriform plate is the only structure separating the nasal cavity from the olfactory bulb in rodents, nasal Oxt administration may activate the Oxt-R present in the olfactory bulb [28, 29]. Second is the route mediated by the AP. c-Fos-ir neurons were increased in the AP after both IP and nasal application of Oxt. The AP is known to have a leaky BBB, and the neurons in the AP project to NTS neurons, which in turn project to the ARC and PVN [30]. Hence, it is possible that nasal and IP injections of Oxt exert their effects on feeding via activating neurons in AP. However, in this study Oxt increased c-Fos-ir neurons in the NTS only after IP injection and not after nasal administration. This may indicate that neural signal transduction through the AP to NTS projection after nasal application of Oxt was not intensive enough to induce c-Fos-ir neurons in the NTS. Third is the route via vagal afferents. In this study, only IP administration of Oxt increased the number of c-Fos-ir neurons in the NTS, where the vagal afferent neurons terminate [31]. Oxt-R is widely expressed in the peripheral tissues including the nodose ganglion [32]. Hence, it is possible that IP-administered Oxt interacts with Oxt-R on the vagal afferent nodose ganglion neurons to signal to the NTS.

Regarding the reduced locomotor activity found only with IP administration of Oxt, the underlying mechanisms could be due to the passage of Oxt from the blood to the brain, thereby activating responsible brain regions, or to the consequences of the peripheral actions of very high levels of Oxt following IP administration. It is important to note that a high peripheral Oxt concentration can also activate vasopressin receptors that have been reported to regulate locomotor activity [33]. Further studies are required to elucidate the mechanism underlying the effect of IP Oxt administration on locomotor activities.

In the present study, nasal and IP administration of Oxt increased the number of c-Fos-ir neurons in the PVN of male mice, suggesting a possible peripheral-central Oxt axis. The result is in agreement with a recent report that the IP administration of Oxt activates PVN Oxt neurons in male rats [34]. Negative feedback effects of Oxt on Oxt neurons were reported under particular conditions in vir-

gin and pregnant female rats, in contrast to positive feedback effects in male and lactating female rats [35–37]. These reports suggest that Oxt activates Oxt neurons in male rodents. Hence, our results could reflect the direct effects of exogenously administered Oxt on PVN Oxt neurons or indirect effects mediated by the nasal/IP Oxt-activated neurons that project to the PVN Oxt neurons.

We have previously reported that chronic Oxt treatment ameliorates the impaired glucose tolerance in high-fat diet-induced obese mice [15]. Since chronic Oxt treatment also ameliorated obesity, the improvement of glucose tolerance by Oxt could be due to its direct effect on glucose metabolism or secondary to the amelioration of obesity. In the present study, IP administration of 40 µg/kg Oxt induced a small effect on food intake but markedly decreased blood glucose levels at 30 min of IPGTT. Furthermore, Oxt elevated plasma insulin level *in vivo* and enhanced glucose-induced insulin secretion in isolated islets *in vitro*. These results taken together suggest that IP-administered Oxt substantially reaches the pancreas and directly interacts with islet β-cells to enhance glucose-induced insulin release, thereby improving glucose tolerance. Insulin, released postprandially [38], might enter the brain and inhibit food intake [27]. It was also reported that insulin activates vagal afferent neurons, which could be linked to the regulation of food intake [39]. Therefore, it is possible that insulin secretion induced by IP Oxt may partly contribute to the anorexic effect of IP Oxt.

In our study, nasal Oxt administration failed to affect glucose tolerance in mice. In dogs, in contrast, nasal Oxt at a similar dose (3–4 µg/kg) was reported to increase plasma insulin and glucagon levels [40]. Also, in humans, nasal administration of Oxt (24 IU) attenuated the elevated blood glucose following the test buffet [17]. The apparent discrepancy in the effect of nasal Oxt on glucose homeostasis could be due to species differences or methodology of treatment as stated above. The nasally administered Oxt might be more easily transferred to the periphery in dogs and humans than in mice.

In order to assess the direct cerebral effect of Oxt on glucose metabolism, we performed the IPGTT after icv injection of Oxt. icv injection of Oxt (0.4, 4 µg/mice) had no effect on glucose metabolism. Although regulation of glucose metabolism through the brain is established, whether this process may be modulated by Oxt is not clear [41, 42]. Our results suggest that Oxt in the brain has little effect on glucose metabolism under the experimental conditions studied here.

When considering the physiological aspect of Oxt on females, it shows different effects on food intake under different conditions. In the preparturition period, Oxt secretion is very low in order to reduce the risk of preterm delivery and to prevent the loss of the accumulating neurophysiological Oxt store [43], which is accompanied by an increase in food intake in both mice and rats [42, 44]. During the parturition and lactation periods, in spite of the extensive activation of Oxt neurons, food intake is dramatically elevated [44]. It is suggested that the involvement of Oxt in feeding behavior is unique in these periods when the energy intake and expenditure are in different states from those in male or virgin animals.

Recent reports have shown that Oxt treatment reduces reward-driven food intake [17]. It is well known that the reward process, including feeding, sexual [45] and social [46] rewards, is related to the mesocorticolimbic dopamine system in the brain [47, 48]. Oxt appears to impact this system [47], in which dopamine is one of the neurotransmitters playing a major role in addiction. It has recently been reported that Oxt modulates the negative aspect of addiction [49] and that Oxt treatment can attenuate the addictive cocaine-seeking behavior in humans [50]. Hyperphagia is considered an addictive behavior for food. The common mechanisms for hyperphagia and addiction have been reported [51]. Therefore, Oxt as a neuropeptide may serve to keep the reward system at a moderate level.

In conclusion, nasal and IP administration of Oxt have similar anorexigenic effects. However, nasal administra-

tion of Oxt may have a lesser effect on the peripheral tissue, including pancreatic  $\beta$ -cells, compared to IP administration. Hence, nasal administration may have the advantage of activating specific brain regions without affecting glucose tolerance and locomotion.

### Acknowledgements

The authors appreciate Dr. Tertina Softley (Oxford UK) for critically reading this paper. This work was supported by Grant-in-Aid for Scientific Research (C) (24591341), Kowa Life Science Foundation, and a research grant of the Astellas Foundation for Research on Metabolic Disorders to Y.M. This study was partly supported by Grant-in-Aid for Scientific Research (B) (23390044), for Challenging Exploratory Research (22659044, 24659101), and for Scientific Research on Innovative Areas (23115715) from the Japan Society for the Promotion of Science (JSPS), Strategic Research Program for Brain Sciences (10036069) by the Ministry of Education, Culture, Sports, Science and Technology of Japan (MEXT), MEXT-Supported Program for the Strategic Research Foundation at Private Universities 2011–2015 (Cooperative Basic and Clinical Research on Circadian Medicine) and 2013–2017, a Grant-in-Aid from Health Labor Sciences Research Grants from the Ministry of Health, Labor, and Welfare, Japan, grants from the Japan Diabetes Foundation, Takeda Science Foundation, and Uehara Memorial Foundation, and Insulin Research Award from Novo Nordisk to T.Y. This study was subsidized by the JKA Foundation through its promotion funds from KEIRIN RACE to T.Y.

### Disclosure Statement

The authors have no conflicts of interest to disclose.

### References

- 1 Kiss A, Mikkelson JD: Oxytocin – anatomy and functional assignments: a minireview. *Endocr Regul* 2005;39:97–105.
- 2 Donaldson ZR, Young LJ: Oxytocin, vasopressin, and the neurogenetics of sociality. *Science* 2008;322:900–903.
- 3 Neumann ID, Landgraf R: Balance of brain oxytocin and vasopressin: implications for anxiety, depression, and social behaviors. *Trends Neurosci* 2012;35:649–659.
- 4 Kosfeld M, Heinrichs M, Zak PJ, Fischbacher, Fehr E: Oxytocin increases trust in humans. *Nature* 2005;435:673–676.
- 5 Feldman R, Weller A, Zagoory-Sharon O, Levine A: Evidence for a neuroendocrinological foundation of human affiliation: plasma oxytocin levels across pregnancy and the postpartum period predict mother-infant bonding. *Psychol Sci* 2007;18:965–970.
- 6 Jin D, Liu HX, Hirai H, Torashima T, Nagai T, Lopatina O, Shnyder NA, Yamada K, Noda M, Seike T, Fujita K, Takasawa S, Yokoyama S, Koizumi K, Shiraiishi Y, Tanaka S, Hashii M, Yoshihara T, Higashida K, Islam MS, Yamada N, Hayashi K, Noguchi N, Kato I, Okamoto H, Matsushima A, Salmina A, Munesue T, Shimizu N, Mochida S, Asano M, Higashida H: CD38 is critical for social behaviour by regulating oxytocin secretion. *Nature* 2007;446:42–45.
- 7 Maejima Y, Sedbazar U, Suyama S, Kohno D, Onaka T, Takano E, Yoshida N, Koike M, Uchiyama Y, Fujiwara K, Yashiro T, Horvath TH, Dietrich MO, Tanaka S, Dezaki K, Oh-I S, Hashimoto K, Shimizu H, Nakata M, Mori M, Yada T: Nesfatin-1-regulated oxytocinergic signalling in the paraventricular nucleus causes anorexia through a leptin-independent melanocortin pathway. *Cell Metab* 2009;10:355–365.
- 8 Olson BR, Drutarosky MD, Chow MS, Hruby VJ, Stricker EM, Verbalis JG: Oxytocin and oxytocin agonist administered centrally decrease food intake in rats. *Peptides* 1991;12:113–118.
- 9 Arletti R, Benelli A, Bertolini A: Oxytocin inhibits food intake and fluid intake in rats. *Physiol Behav* 1990;48:825–830.
- 10 Takayanagi Y, Kasahara Y, Onaka T, Takahashi N, Kawada T, Nishimori K: Oxytocin receptor-deficient mice developed late-onset obesity. *Neuroreport* 2008;9:951–955.
- 11 Camerino C: Low sympathetic tone and obese phenotype in oxytocin-deficient mice. *Obesity (Silver Spring)* 2009;17:980–984.
- 12 Ogden CL, Kit BK, Carroll MD, Flegal KM: Prevalence of obesity and trends in body mass index among US children and adolescents, 1999–2010. *JAMA* 2012;307:483–490.

- 13 Bardou M, Barkun AN, Martel M: Obesity and colorectal cancer. *Gut* 2013;62:933–947.
- 14 Suplicy H, Boguszewski CL, Dos Santos CM, do Desterro de Figueiredo M, Cunha DR, Radominski R: A comparative study of five centrally acting drugs on the pharmacological treatment of obesity. *Int J Obes (Lond)* 2014; 38:1097–1103.
- 15 Maejima Y, Iwasaki Y, Yamahara Y, Kodaira M, Sedbazar U, Yada T: Peripheral oxytocin treatment ameliorates obesity by reducing food intake and visceral fat mass. *Aging (Albany NY)* 2011;3:1169–1177.
- 16 Zhang H, Wu C, Chen Q, Chen X, Xu Z, Wu J, Cai D: Treatment of obesity and diabetes using oxytocin or analogs in patients and mouse models. *PLoS One* 2013;8:1–11.
- 17 Ott V, Finlayson G, Lehnert H, Heitmann B, Heinrichs M, Born J, Hallschmid M: Oxytocin reduces reward-driven food intake in humans. *Diabetes* 2013;62:3418–3425.
- 18 Shimomura K, Galvanovslis J, Goldsworthy M, Hugill A, Kaizak S, Lee A, Meadows N, Quwailid MM, Rydström J, Teboul L, Ashcroft F, Cox RD: Insulin secretion from beta-cells is affected by deletion of nicotinamide nucleotide transhydrogenase. *Methods Enzymol* 2009;457:451–480.
- 19 Neumann ID, Maloumy R, Beiderbeck DI, Lukas M, Landgraf R: Increased brain and plasma oxytocin after nasal and peripheral administration in rats and mice. *Psychoneuroendocrinology* 2013;38:1985–1993.
- 20 Ramos L, Hicks C, Caminer A, McGregor IS: Inhaled vasopressin increases sociability and reduces body temperature and heart rate in rats. *Psychoneuroendocrinology* 2014;46:46–51.
- 21 Mens WB, Witter A, Van Wismersm Greidanus TB: Penetration of neurophysal hormones from plasma into cerebrospinal fluid (CSF): half-times of disappearance of these neuropeptides from CSF. *Brain Res* 1983;262: 143–149.
- 22 Banks WA, Kastin AJ: Passage of peptides across the blood-brain barrier: pathophysiological perspectives. *Life Sci* 1996;59:1923–1943.
- 23 Ludwig M, Tobin VA, Callahan MF, Papadaki E, Becker A, Engelmann M, Leng G: Intranasal application of vasopressin fails to elicit changes in brain immediate early gene expression. Neural activity and behavioral performance of rats. *J Neuroendocrinol* 2013;25: 655–667.
- 24 Bridges TE, James NV: The hypothalamo-neurohypophysial system of native Australian desert rodents. The vasopressin and oxytocin contents of hypothalamus and posterior pituitary of *Notomys alexis* and *Pseudomys australis* compared with those of the laboratory rat and mouse in different states of water balance. *Aust J Exp Biol Med Sci* 1982;60: 265–283.
- 25 Swanson LW, Sawchenko PE: Hypothalamic integration: organization of the paraventricular and supraoptic nuclei. *Annu Rev Neurosci* 1983;6:269–324.
- 26 Xu Y, Wu Z, Sun H, Zhu Y, Kim ER, Lowell BB, Arenkiel BR, Xu Y, Tong Q: Glutamate mediates the function of melanocortin receptor 4 on Sim1 neurons in body weight regulation. *Cell Metab* 2013;18:860–870.
- 27 Schwartz MW, Woods SC, Porte D Jr, Seeley RJ, Baskin DG: Central nervous system control of food intake. *Nature* 2000;404:661–671.
- 28 Putheti RR, Patil MC, Obire O: Nasal drug delivery in pharmaceutical and biotechnology: present and future. *J Sci Technol* 2009;4:1–21.
- 29 Gould BR, Zingg HH: Mapping oxytocin receptor gene expression in the mouse brain and mammary gland using an oxytocin receptor-lacZ reporter mouse. *Neuroscience* 2003; 122:155–168.
- 30 Stein MK, Loewy AD: Area postrema projects to FoxP2 neurons of the pre-locus and parabrachial nuclei: brainstem sites implicated in sodium appetite regulation. *Brain Res* 2010;1359:116–127.
- 31 Browning KN, Travaglini RA: Plasticity of vagal brainstem circuits in the control of gastrointestinal function. *Auton Neurosci* 2011;161: 6–13.
- 32 Welch MG, Tamir H, Gross KJ, Chen J, Anwar M, Gershon MD: Expression and developmental regulation of oxytocin (OT) and oxytocin receptors (OTR) in the enteric nervous system (ENS) and intestinal epithelium. *J Comp Neurol* 2009;512:265–270.
- 33 Cormier HC, Della-Maggiore V, Karatsoreos IN, Koletar MM, Ralph MR: Suprachiasmatic vasopressin and the circadian regulation of voluntary locomotor behavior. *Eur J Neurosci* 2015;41:79–88.
- 34 Zhang G, Cai D: Circadian intervention of obesity development via resting-stage feeding manipulation or oxytocin treatment. *Am J Physiol Endocrinol Metab* 2011;301:E1004–E1012.
- 35 Moos F, Freund-Mercier MJ, Guerné Y, Guerné JM, Stoessel ME, Richard P: Release of oxytocin and vasopressin by magnocellular nuclei in vitro: specific facilitatory effect of oxytocin on its own release. *J Endocrinol* 1984;102:63–72.
- 36 Neumann J, Koehler E, Landgraf R, Summy-Long J: An oxytocin receptor antagonist infused into the supraoptic nucleus attenuates intranuclear and peripheral release of oxytocin during suckling in conscious rats. *Endocrinology* 1994;134:141–148.
- 37 Kawarabayashi T, Kuriyama K, Nakashima T, Kiyohara T, Sugimori H: Oxytocin modulates oxytocin neurons in the paraventricular nuclei of female rats throughout pregnancy and parturition. *Am J Obstet Gynecol* 1993;168: 969–974.
- 38 Cummings DE, Purnell JQ, Frayo RS, Schimidova K, Wisse BE, Weigle DS: A preprandial rise in plasma ghrelin levels suggests a role in meal initiation in humans. *Diabetes* 2001;50: 1714–1719.
- 39 Iwasaki Y, Shimomura K, Kohno D, Dezaki K, Ayush EA, Nakabayashi H, Kubota N, Kadowaki T, Kakei M, Nakata M, Yada T: Insulin activates vagal afferent neurons including those innervating pancreas via insulin cascade and Ca<sup>2+</sup> influx: its dysfunction in IRS2-KO mice with hyperphagic obesity. *PLoS One* 2013;8:e67198.
- 40 Altszuler N, Hampshire J: Intranasal instillation of oxytocin increases insulin and glucagon secretion. *Proc Soc Exp Biol Med* 1981; 168:123–124.
- 41 Schwartz MW, Seeley RJ, Tschöp MH, Woods SC, Morton GJ, Myers MG, D'Alessio D: Cooperation between brain and islet in glucose homeostasis and diabetes. *Nature* 2013;503: 59–66.
- 42 Björkstrand E, Eriksson M, Uvnäs-Moberg K: Evidence of a peripheral and a central effect of oxytocin on pancreatic hormone release in rats. *Neuroendocrinology* 1996;63: 377–383.
- 43 Douglas AJ, Johnstone LE, Leng G: Neuroendocrine mechanisms of change in food intake during pregnancy: a potential role for brain oxytocin. *Physiol Behav* 2007;24:352–365.
- 44 Makarova EN, Kochubei ED, Bazhan NM: Regulation of food consumption during pregnancy and lactation in mice. *Neurosci Behav Physiol* 2010;40:263–267.
- 45 Argiolas A, Melis MR: The role of oxytocin and the paraventricular nucleus in the sexual behaviour of male mammals. *Physiol Behav* 2004;83:309–317.
- 46 Young KA, Liu Y, Gobrogge KL, Wang H, Wang Z: Oxytocin reverses amphetamine-induced deficits in social bonding: evidence for an interaction with nucleus accumbens dopamine. *J Neurosci* 2014;34:8499–8506.
- 47 Love TM: Oxytocin, motivation and the role of dopamine. *Pharmacol Biochem Behav* 2014;119:49–60.
- 48 Gimpl G, Fahrenholz F: The oxytocin receptor system: structure, function, and regulation. *Physiol Rev* 2001;81:629–683.
- 49 McGregor IS, Bowen MT: Breaking the loop: oxytocin as a potential treatment for drug addiction. *Horm Behav* 2012;61:331–339.
- 50 Morales-Rivera A, Hernández-Burgos MM, Martínez-Rivera A, Pérez-Colón J, Rivera R, Montalvo J, Rodríguez-Borrero E, Maldonado-Vlaar CS: Anxiolytic effects of oxytocin in cue-induced cocaine seeking behavior in rats. *Psychopharmacology (Berl)* 2014;231:4145–4155.
- 51 Kenny PJ: Common cellular and molecular mechanisms in obesity and drug addiction. *Nat Rev Neurosci* 2011;12:638–651.



## Original article

## Microarray analysis of 50 patients reveals the critical chromosomal regions responsible for 1p36 deletion syndrome-related complications

Shino Shimada<sup>a,b</sup>, Keiko Shimojima<sup>a</sup>, Nobuhiko Okamoto<sup>c</sup>, Noriko Sangu<sup>a,d</sup>,  
Kyoko Hirasawa<sup>b</sup>, Mari Matsuo<sup>e</sup>, Mayo Ikeuchi<sup>f</sup>, Shuichi Shimakawa<sup>g</sup>,  
Kenji Shimizu<sup>h</sup>, Seiji Mizuno<sup>i</sup>, Masaya Kubota<sup>j</sup>, Masao Adachi<sup>k</sup>,  
Yoshiaki Saito<sup>l</sup>, Kiyotaka Tomiwa<sup>m</sup>, Kazuhiro Haginoya<sup>n</sup>, Hironao Numabe<sup>o</sup>,  
Yuko Kako<sup>p</sup>, Ai Hayashi<sup>q</sup>, Haruko Sakamoto<sup>r</sup>, Yoko Hiraki<sup>s</sup>, Koichi Minami<sup>t</sup>,  
Kiyoshi Takemoto<sup>u</sup>, Kyoko Watanabe<sup>v</sup>, Kiyokuni Miura<sup>w</sup>,  
Tomohiro Chiyonobu<sup>x</sup>, Tomohiro Kumada<sup>y</sup>, Katsumi Imai<sup>z</sup>,  
Yoshihiro Maegaki<sup>aa</sup>, Satoru Nagata<sup>b</sup>, Kenjiro Kosaki<sup>ab</sup>,  
Tatsuro Izumi<sup>f</sup>, Toshiro Nagai<sup>ac</sup>, Toshiyuki Yamamoto<sup>a,\*</sup>

<sup>a</sup> Tokyo Women's Medical University Institute for Integrated Medical Sciences, Tokyo, Japan

<sup>b</sup> Department of Pediatrics, Tokyo Women's Medical University, Tokyo, Japan

<sup>c</sup> Department of Medical Genetics, Osaka Medical Center and Research Institute for Maternal and Child Health, Izumi, Japan

<sup>d</sup> Department of Oral and Maxillofacial Surgery, School of Medicine, Tokyo Women's Medical University, Tokyo, Japan

<sup>e</sup> Institute of Medical Genetics, Tokyo Women's Medical University, Tokyo, Japan

<sup>f</sup> Department of Pediatrics and Child Neurology, Oita University Faculty of Medicine, Oita, Japan

<sup>g</sup> Department of Pediatrics, Osaka Medical College, Takatsuki, Japan

<sup>h</sup> Division of Medical Genetics, Saitama Children's Medical Center, Saitama, Japan

<sup>i</sup> Department of Pediatrics, Central Hospital, Aichi Human Service Center, Kasugai, Japan

<sup>j</sup> Division of Neurology, National Center for Child Health and Development, Tokyo, Japan

<sup>k</sup> Department of Pediatrics, Kakogawa Hospital Organization, Kakogawa West-City Hospital, Kakogawa, Japan

<sup>l</sup> Department of Child Neurology, National Center of Neurology and Psychiatry, Tokyo, Japan

<sup>m</sup> Department of Pediatrics, Medical Center for Children, Osaka City General Hospital, Osaka, Japan

<sup>n</sup> Department of Pediatric Neurology, Takuto Rehabilitation Center for Children, Sendai, Japan

<sup>o</sup> Department of Genetic Counseling, Graduate School of Humanities and Sciences, Ochanomizu University, Tokyo, Japan

<sup>p</sup> Department of Pediatrics, Showa University School of Medicine, Tokyo, Japan

<sup>q</sup> Department of Neonatology, Japanese Red Cross Kyoto Daiichi Hospital, Kyoto, Japan

<sup>r</sup> Department of Pediatrics, Osaka Red Cross Hospital, Osaka, Japan

<sup>s</sup> Hiroshima Municipal Center for Child Health and Development, Hiroshima, Japan

<sup>t</sup> Department of Pediatrics, Wakayama Medical University, Wakayama, Japan

<sup>u</sup> Osaka Developmental Rehabilitation Center, Osaka, Japan

<sup>v</sup> Department of Pediatrics, National Hospital Organization Kokura Medical Center, Kitakyushu, Japan

<sup>w</sup> Developmental Disability Medicine, Nagoya University Graduate School of Medicine, Nagoya, Japan

<sup>x</sup> Department of Pediatrics, Graduate School of Medical Science, Kyoto Prefectural University of Medicine, Kyoto, Japan

<sup>y</sup> Department of Pediatrics, Shiga Medical Center for Children, Moriyama, Japan

<sup>z</sup> National Epilepsy Center, Shizuoka Institute of Epilepsy and Neurological Disorders, Shizuoka, Japan

\* Corresponding author. Address: Tokyo Women's Medical University Institute for Integrated Medical Sciences, 8-1 Kawada-cho, Shinjuku-ward, Tokyo 162-8666, Japan. Tel.: +81 3 3353 8111x24013; fax: +81 3 5269 7667.

E-mail address: yamamoto.toshiyuki@twmu.ac.jp (T. Yamamoto).

<http://dx.doi.org/10.1016/j.braindev.2014.08.002>

0387-7604/© 2014 The Japanese Society of Child Neurology. Published by Elsevier B.V. All rights reserved.

Please cite this article in press as: Shimada S et al. Microarray analysis of 50 patients reveals the critical chromosomal regions responsible for 1p36 deletion syndrome-related complications. Brain Dev (2014), <http://dx.doi.org/10.1016/j.braindev.2014.08.002>

<sup>aaa</sup> Division of Child Neurology, Tottori University School of Medicine, Yonago, Japan<sup>ab</sup> Center for Medical Genetics, Keio University School of Medicine, Tokyo, Japan<sup>ac</sup> Department of Pediatrics, Dokkyo Medical University Koshigaya Hospital, Saitama, Japan

Received 2 April 2014; received in revised form 1 August 2014; accepted 5 August 2014

## Abstract

**Objective:** Monosomy 1p36 syndrome is the most commonly observed subtelomeric deletion syndrome. Patients with this syndrome typically have common clinical features, such as intellectual disability, epilepsy, and characteristic craniofacial features.

**Method:** In cooperation with academic societies, we analyzed the genomic copy number aberrations using chromosomal microarray testing. Finally, the genotype–phenotype correlation among them was examined.

**Results:** We obtained clinical information of 86 patients who had been diagnosed with chromosomal deletions in the 1p36 region. Among them, blood samples were obtained from 50 patients (15 males and 35 females). The precise deletion regions were successfully genotyped. There were variable deletion patterns: pure terminal deletions in 38 patients (76%), including three cases of mosaicism; unbalanced translocations in seven (14%); and interstitial deletions in five (10%). Craniofacial/skeletal features, neurodevelopmental impairments, and cardiac anomalies were commonly observed in patients, with correlation to deletion sizes.

**Conclusion:** The genotype–phenotype correlation analysis narrowed the region responsible for distinctive craniofacial features and intellectual disability into 1.8–2.1 and 1.8–2.2 Mb region, respectively. Patients with deletions larger than 6.2 Mb showed no ambulation, indicating that severe neurodevelopmental prognosis may be modified by haploinsufficiencies of *KCNAB2* and *CHD5*, located at 6.2 Mb away from the telomere. Although the genotype–phenotype correlation for the cardiac abnormalities is unclear, *PRDM16*, *PRKCZ*, and *RERE* may be related to this complication. Our study also revealed that female patients who acquired ambulatory ability were likely to be at risk for obesity.

© 2014 The Japanese Society of Child Neurology. Published by Elsevier B.V. All rights reserved.

**Keywords:** 1p36 deletion syndrome; Chromosomal deletion; Genotype–phenotype correlation; Intellectual disability; Ambulation; Epilepsy; Distinctive features

## 1. Introduction

Monosomy 1p36 syndrome is a congenital malformation syndrome caused by the subtelomeric deletion of the short arm of chromosome 1 [1–3]. This syndrome is the most commonly observed subtelomere deletion syndrome, with an estimated incidence of 1:5000–1:10,000 [4,5]. Patients with this syndrome exhibit common clinical features, including intellectual disability (ID) and characteristic craniofacial features; such as straight eyebrows, deep-set eyes, epicanthus, and a pointed chin [6–9]. Although the levels of ID vary among patients, craniofacial features are commonly seen [10]. The patients with the 1p36 deletion syndrome also show many other complications, including hypotonia, seizures, hearing loss, structural heart defects, cardiomyopathy, ophthalmological abnormalities, and behavior abnormalities [7]. Recent advances in microarray-based chromosomal testing have helped us to identify small chromosomal rearrangements that are invisible by conventional G-banded chromosomal tests/karyotyping [11,12]. Using this method, the precise locations of the aberrations can be revealed at the molecular level. These advances have also allowed the study of more in-depth genotype–phenotype correlations for this syndrome, as

well as the identification of some of the regions responsible for individual complications [12,13].

In this study, we performed a nation-wide survey for the 1p36 deletion syndrome in Japan. The aim of this study was to identify the chromosomal regions responsible for individual complications in patients with 1p36 deletions. We analyzed the affected genomic regions in 50 patients with 1p36 deletions, and performed correlational analyses of the genotype data with the clinical information.

## 2. Materials and methods

### 2.1. Patients and samples

We performed a nation-wide survey for the 1p36 deletion syndrome with the cooperation of two academic societies; the Japanese Society of Child Neurology and the Japan Society of Pediatric Genetics. The study subjects were Japanese patients who had already been diagnosed using various diagnostic methods, including conventional karyotyping, subtelomere fluorescence *in situ* hybridization (FISH) analysis, multiplex ligation-dependent probe amplification (MLPA), and chromosomal microarray testing. Five patients



(patient [Pt] 8, 9, 21, 28, and 43), whose clinical features have been previously reported [14–17], were also included in this study. With the questionnaire survey for attending physicians, we accumulated the patients' clinical information, including craniofacial/skeletal features, neurodevelopmental features, brain structural abnormalities, cardiac abnormalities, sensory-organs abnormalities, urogenital abnormalities, endocrinological and nutritional findings among others. This study was approved by the ethics committee in Tokyo Women's Medical University.

On receipt of written informed consents from the families of the patients, we obtained the patients' blood samples to determine genomic copy number losses in the patients. Genomic DNA was extracted from the blood samples using the QIA quick DNA Extraction Kit (QIAGEN, Hamburg, Germany). Metaphase spreads were also prepared from blood samples and used for FISH analyses. In cases, if we could obtain written informed consent, parental samples were also analyzed.

## 2.2. Molecular and cytogenetic analyses

Chromosomal microarray testing was performed using any of the Agilent Oligo Microarray Kits 44, 60, 105, 180, and 244 K (Agilent Technologies, Santa Clara, CA), as described previously [18,19]. Genomic copy number aberrations were visualized using Agilent Genomic Workbench version 6.5 (Agilent Technologies). For cases in which variations of unknown significance were identified or suspected, parental samples were also analyzed. In cases of complex chromosomal rearrangements or mosaicism, metaphase spreads prepared using the patients' samples were used for FISH analyses for confirmation. The bacterial artificial clones were selected from the UCSC genome browser (<http://genome.ucsc.edu/>) for use as probes. For the target probes, RP11-425E15 (1p36.33: 949,400–1,132,489), RP11-82D16 (1p36.33: 2,046,751–2,208,312), RP11-70N12 (1p36.32: 2,740,703–2,922,551), CTD-3209F18 (1p36.32: 3,530,092–3,769,006), and RP11-933B18 (1p36.31: 5,988,719–6,177,261) were selected, while CTB-167K11 (1q44: 249,250,621–249,250,621) was used as a marker of chromosome 1. All of the genomic regions are described according to the February 2009 human reference sequence (GRCh37/hg19) in this study.

## 3. Results

### 3.1. Molecular-cytogenetic findings

We obtained clinical information from 86 patients with chromosomal deletions involving 1p36 regions. Among them, 50 patients (15 males and 35 females) were successfully genotyped. All of the genotypes were summarized in Tables 1 and 2, and 1p36 deletions identified

in the patients were depicted in the genome map (Fig. 2). The minimum and maximum deletion sizes was 0.9 and 12.9 Mb, respectively. Pure terminal deletions were identified in 38 patients (76%). Among them, three patients (Pt 8, 19, and 21) exhibited mosaicism. Pt 8 was first diagnosed with mosaic 1p36 deletion by chromosomal microarray testing, and Pt 21 had been diagnosed with 1p36 deletion using subtelomere FISH analysis; however, mosaicism was not reported at that time [17]. Although the mosaic deletion of 1p36 in Pt 19 had been firstly confirmed by FISH, we could not detect the breakpoint by chromosomal microarray testing due to low frequency (28% mosaic ratio). As the breakpoint was determined to be between two FISH probes (CTD-3209F18 and RP11-933B18), the proximal end of CTD-3209F18 was used as the minimum deletion region in this patient.

Additional aberrations with the sizes over 0.5 Mb were identified in eight patients (Pt 2, 10, 11, 15, 20, 28, 34, and 43) involving chromosomes 4, 7, 8, 13, and Y (Table 2), including a possible benign copy number aberration in Pt 15, which was also observed in the healthy mother. The other seven patients were confirmed to have unbalanced translocations by cytogenetic evaluation (14%), using either G-banding or FISH analysis. Two translocations were diagnosed as *de novo*, and the others were designated as unknown because of the lack of availability of parental information.

Five patients (Pt 1, 14, 47, 48, and 50) had interstitial deletions (10%) with a deletion size between 0.9 and 10.3 Mb.

### 3.2. Clinical findings

Clinical information of the 50 patients successfully genotyped is summarized in Table 3. Estimated frequencies of each complication are also included in Table 3. Pt 26 and 49 suddenly died at 24 and 10 months old of age, respectively. Pt 49 probably died due to heart failure but Pt 26 died of an unknown cause (detailed information unavailable).

#### 3.2.1. Craniofacial features

Most of the patients showed craniofacial features, including straight eyebrows (84%), deep-set eyes (93%), broad nasal bridge (97%), low set ears (88%), and a pointed chin (89%). Constellations of these findings make distinctive facial impressions for 1p36 deletion syndrome, observed in Pt 3, 6, and 14 (Fig. 1b–d). This observation suggests that hypotelorism is rather characteristic among these patients. On the other hand, Pt 1 did not show deep-set eyes (Fig. 1a). The craniofacial features of three patients (Pt 47, 48, and 50) did not exhibit hypotelorism (Fig. 2e–g). From the genotypic point of view, these three patients (Pt 47, 48, and 50) would be diagnosed as having the proximal 1p36 deletion syndrome [20,21].

Table 1  
The ranges of 1p36 deletions analyzed by chromosomal microarray testing.

Patient number	Age (year)	Gender	Platform (k)	Start <sup>a</sup>	End <sup>a</sup>	Additional aberration	FISH probe	Mosaic ratio <sup>b</sup> (%)	References
1	14	F	180	834,101	1,770,669	Interstitial	RP11-425E15		
2	9	M	44	1	1,820,584	der(1)t(Y;1), idic(Y)			
3	6	F	180	1	2,186,829				
4	1	F	60	1	2,239,497				
5	3	F	44	1	2,281,699				
6	5	F	60	1	2,553,982				
7	2	M	60	1	2,553,982				
8	5	F	44	1	3,044,953	Mosaicism	RP11-82D16	70	Shimada et al. [17]
9	13	F	44	1	3,102,718				Okamoto et al. [14]
10	18	F	44	1	3,102,718	der(1)t(1;7)			
11	17	F	60	1	3,138,565	der(1)t(1;8)			
12	8	F	60	1	3,265,702				
13	11	F	244	1	3,408,152				
14	5	M	60	1,786,789	3,472,907	Interstitial			
15	2	F	180	1	3,564,328				
16	13	M	60	1	3,582,084				
17	4	F	44	1	3,607,275				
18	2	F	60	1	3,660,110				
19	3	F	60	1	3,769,006	Mosaicism	CTD-3209F18	28	
20	3	M	44	1	4,070,842	der(1)t(1;13)			
21	17	F	44	1	4,481,324	Mosaicism	RP11-82D16	77	Shimada et al. [17]
22	2	F	180	1	4,703,581				
23	6	M	60	1	4,779,157				
24	3	F	60	1	4,843,370				
25	6	F	44	1	4,843,718				
26	2	M	60	1	5,252,985				
27	0	F	44	1	5,252,985				
28	25	F	44	1	5,411,803	der(1)t(Y;1)			Hiraki et al. [15]
29	3	F	44	1	6,128,223				
30	3	F	60	1	6,282,562				
31	1	F	60	1	6,282,562				
32	3	M	60	1	6,882,431				
33	7	M	60	1	7,035,075				
34	1	F	60	1	7,187,535	der(1)t(1;4)			
35	10	M	60	1	7,392,688				
36	8	M	60	1	7,581,058				
37	3	F	44	1	8,077,959				
38	2	F	60	1	8,104,671				
39	3	M	44	1	8,104,671				
40	4	M	44	1	8,181,042				
41	5	F	44	1	8,181,042				
42	1	F	60	1	8,427,633				
43	3	M	60	1	9,180,975	der(1)(1;4)			Saito et al. [16]
44	5	F	60	1	9,251,936				
45	4	M	60	1	9,953,030				

46	2	F	44	1	10,001,011	Interstitial
47	4	F	44	2,080,309	10,869,155	Interstitial
48	8	F	60	2,785,042	12,743,178	Interstitial
49	0	F	44	1	12,917,483	Interstitial
50	22	F	180	6,614,950	16,890,814	Interstitial

<sup>a</sup> The genomic position referring build19.

<sup>b</sup> The mosaic ratio was confirmed by FISH; F, female; M, male.

### 3.2.2. Neurological features

Almost all patients showed ID (98%) but a patient (Pt 2) having a deletion in the far distal region of 1p36 showed borderline ID, with an intelligence quotient (IQ) of 80. Therefore, this region could be eliminated from the responsible region for ID (Fig. 2). The smallest deletion, an interstitial deletion between genomic positions 0.8 and 1.8 Mb, was identified in Pt 1 (Fig. 2). In spite of having this smallest deletion, Pt 1 had severe ID, i.e., she was locomotive but aphasic and required support for all activities in her daily life. This was probably a consequence of intractable epilepsy associated with tonic seizures, caused by factors other than the interstitial deletion of this region. The proximal and distal ends of the breakpoints in Pt 3 and 14 defined the shortest region of overlap for ID, spanning the 1.8–2.2 Mb region (Fig. 2; region B). Axial hypotonia (92%) and poor sucking (70%) were also commonly observed. Epilepsy, one of the major complications in 1p36 deletion syndrome, was observed in 70% of the patients. Infantile spasms were observed in 16% of the patients.

In this study, many types of structural brain abnormalities were identified; not only in the cerebral cortex but also in the white matter (Table 3), indicating that there is no major pattern. The most frequently observed abnormality was a nonspecific finding with enlargement of lateral ventricles.

### 3.2.3. Cardiac abnormality

Cardiac abnormality is one of the most frequently observed complications in patients with 1p36 deletions. In this study, congenital heart defects and functional abnormalities were observed in 69% (34/49) and 22% (11/49) of the patients, respectively. The most frequently observed patterns were patent ductus arteriosus (PDA; 37% [18/49]) and ventricular septal defects (VSD; 37% [18/49]).

### 3.2.4. Other complications

Many kinds of complications were observed in many organs. Cryptorchidism was the most frequently observed complication in male patients (64% [9/14]). As Pt 14, with a small interstitial deletion spanning from 1.8 to 3.5 Mb, had cryptorchidism, the deleted region was likely involved in abnormalities of the external genitalia (Fig. 2; region H). Hearing problems (39% [19/49]) and strabismus (33% [15/46]) were relatively common among the patients. Obesity was observed in 5 patients (11% [5/46]).

Renal abnormalities were rare and identified only in three patients. Among them, Pt 26, who had a 5.3 Mb deletion, was diagnosed with the autosomal recessive cystic kidney disease of nephronophthisis (this patient died at 2 years of age) [22]. One of the genes responsible for this condition, the nephronophthisis 4 gene

Table 2  
Additional aberrations identified in the patients.

Patient number	Chr	Start <sup>a</sup>	End <sup>a</sup>	Remark	Attribute	Origin
2	Y	1	59,373,566	der(1)t(Y;1)(p36.3;q12), idic(Y)(q12)	dup	NA
10	7	1	6,870,943	der(1)t(1;7)(p36.32;p22.1)	dup	NA
11	8	1	3,909,039	der(1)t(1;8)(p36.22;p23.2)	dup	NA
15	1	146,324,068	149,192,104	del(1)(q21.1;q21.2)	del	Common with mother
20	13	100,462,233	115,169,878	der(1)t(1;13)(p26.32;q32.3)	dup	De novo
28	Y	26,435,039	59,373,566	der(1)t(Y;1)(q12;p36.32) <sup>#</sup>	dup	NA
34	4	1	13,396,747	der(1)t(1;4)(p36.31;p15.33)	dup	De novo
43	4	189,012,426	191,154,276	der(1)t(1;4)(p36.31;q35.2)	dup	NA

<sup>a</sup> The genomic position referring build19; dup, duplication; del, deletion; NA, not available.

<sup>#</sup> This case was previously reported by Hiraki et al. [15].

(*NPHP4*), is located on 1p36 (chr1: 5,946,555–5,965,543) [23], proximal to the deletion region of three patients with renal abnormalities (Pt 26, 33, and 35). It is unclear whether there is a correlation between *NPHP4* and the renal abnormalities observed in this study.

#### 4. Discussion

##### 4.1. Previous genetic studies on the 1p36 deletion syndrome

Many cohort studies have been performed to delineate the phenotypic features of patients with 1p36 deletion syndrome and to evaluate the frequency of complications [1,6,7]. It has been reported that there is no correlation between the deletion size and the number of observed clinical features [24], while the critical region responsible for core phenotypic features, including clefting, hypothyroidism, cardiomyopathy, hearing loss, large fontanel, and hypotonia, has been narrowed down to a region 2.2 Mb from the telomere [3]. Compared to such core phenotypic features, other complications tend to vary with the size of the deletion, and study subjects with larger deletions tend to have more phenotypic features [25], suggesting that the various phenotypic features are dependent on genes involved in the deletion regions. Thus, precise knowledge of the genotype–phenotype correlations could potentially lead to more personalized treatments for individuals with 1p36 deletions and might identify mutations for single gene disorders [3]. The potassium voltage-gated channel, shaker-related subfamily, beta member 2 gene (*KCNAB2*) and the v-ski sarcoma viral oncogene homolog gene (*SKI*) were identified as candidate genes for the epilepsy phenotype and clefting abnormalities, respectively [26,27]. More recently, the PR domain containing 16 gene (*PRDM16*) was identified as a possible candidate gene for cardiomyopathy, as *PRDM16* was included in a minimal deletion among patients with 1p36 deletions associated with cardiomyopathy, while in patients with pure cardiomyopathy, single nucleotide variants

of *PRDM16* were identified as the cause of cardiomyopathy [28]. This was one of the most successful studies of genotype–phenotype correlation in patients with 1p36 deletions [28].

##### 4.2. Craniofacial features

As mentioned above, a region 2.2 Mb from the telomere has been reported to be responsible for core phenotypic features of 1p36 deletion syndrome [3]. Compared to this, we observed atypical facial features in four patients (Pt 1, 47, 48, and 50) whose deletions did not include the 1.8–2.1 Mb region, in this study. Thus, the region responsible for typical facial features is narrowed into this region (Fig. 2; region A). Because hypotelorism has never been listed in the clinical delineations of 1p36 deletion syndrome reported from Western countries, we did not include this finding in the questionnaire survey and the frequency of this finding in Japanese patients could not be calculated. However, it is commonly observed in Japanese patients with typical 1p36 deletion syndrome. Therefore, hypotelorism may be a characteristic finding among Asian patients.

##### 4.3. Neurological features

Although more severe ID was reported to be associated with larger 1p36 deletions [10], the genomic region responsible for severe ID has never been identified. In this study, a patient (Pt 28) having a 5.4 Mb deletion acquired independent gait, while patients with >6.1 Mb deletions had not yet acquired independent gait, and exhibited severe ID. Thus, the region between 5.4 and 6.1 Mb would appear to be the borderline for independent gait (Fig. 2; region C), and the modifier genes for prognosis of development may be located in the region proximal to this borderline. *KCNAB2*, mentioned above, may be one of the modifier genes responsible for severe ID. Chromodomain helicase DNA-binding protein 5 (*CHD5*; chr1: 6,161,847–6,240,194), which encodes a neuron-specific protein, is